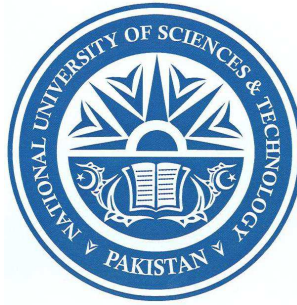


Numerical Solutions of Boundary Layer Flows with Variable Fluid Properties

by

Shafaq Naz



Supervised by

Dr. Muhammad Asif Farooq


School of Natural Sciences(SNS),
National University of Sciences and Technology(NUST),
Islamabad, Pakistan

A thesis submitted for the degree of
Master of Philosophy in Mathematics

© Shafaq Naz 2016

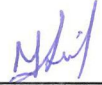
National University of Sciences & Technology**MASTER'S THESIS WORK**

We hereby recommend that the dissertation prepared under our supervision by: Shafaq Naz, Regn No. NUST201463621MSNS78014F Titled: Numerical Solutions of Boundary Layer Flow with Variable Fluid Properties be accepted in partial fulfillment of the requirements for the award of **MS** degree.

Examination Committee Members1. Name: Dr. Meraj Mustafa HashmiSignature: 2. Name: Dr. Mujeeb ur RehmanSignature: 

3. Name: _____

Signature: _____

4. Name: Dr. Nasir AliSignature: Supervisor's Name: Dr. Muhammad Asif FarooqSignature: 


 Head of Department

17-08-16

 Date
COUNTERSIGNEDDate: 17/8/16


 Dean/Principal

Acknowledgements

All glory be to **Almighty Allah**, the most merciful and the benevolent and His beloved **Prophet Muhammad (P.B.U.H)**. This dissertation is written in one year of M. Phil. research phase at NUST-SNS, Islamabad, Pakistan.

I would like to express my deepest gratitude to my parents (especially my late father Muhammad Iqbal), grandfather Muhammad Anwar, uncles Muhammad Masood, Muhammad Navid, Muhammad Rauf and younger brothers Muhammad Deen, and Hassnain Ali for their continuous support (financial and moral), sincere prayers, encouragement, care and patience during my studies. I also owe much to my mother, without her love, encouragement and prayers I would not have completed this work.

I would also like to express my special thanks and gratitude to my supervisor Dr. Muhammad Asif Farooq for his wonderful support, guidance and encouragement to complete my Mphil research. Without his constant support and guidance, completion of this tough journey would not have been possible at all.

Secondly, I would also like to pay my regards to my GEC committee members, Dr. Meeraj Mustafa and Dr. Mujeeb-ur- Rehman who have always encouraged me for quality of the work. Their helpful comments have improved my work day by day. I am also grateful to the HOD Mathematics Dr. Matloob Anwar, Principal Dr. Azad Akhter Siddique and all faculty members of Mathematics department, for helping me during my whole Mphil program. I would also like to thank my friends Amna Khalil, Ismat jabeen, Hafsa inam for their valuable assistance, help and prayers, and the staff of School of Natural sciences (SNS).

Last but not the least, I would like to thank National University of Sciences and Technology (NUST) for providing me with special scholarship to support my studies.

Shafaq Naz

Abstract

In this thesis, we study the variable fluid properties of a boundary layer flow on a moving flat plate in a parallel free stream and the MHD stagnation-point flow and heat characteristics are studied for the stretching sheet case. For a viscous fluid, the MHD boundary layer flow and heat transfer with variable viscosity using power law is also discussed. The numerical solutions for the MHD flow are applied. Constant fluid properties, the variable viscosity, and the exponential temperature dependent cases are considered for the solutions of the flow problems.

We reduced the system of governing nonlinear partial differential equations (PDEs) into nonlinear coupled ordinary differential equations (ODEs) by using the similarity transformations. Results for the solutions are computed by using the shooting technique and are compared with the *bvp4c*, a built-in solver of MATLAB. The numerical results for the variation of different values of velocity, temperature, skin friction coefficient, and the Nusselt number are analyzed. The effects for the different values of the parameters on the velocity and temperature profiles are plotted and discussed in tabular form as well. Results of the fluid that are obtained with the variable properties are different when compared with the constant fluid properties.

Preface

This thesis constitutes five chapters. In the first chapter the basic concepts, definitions, and terminologies related to fluids are presented. A brief description of the shooting method and *bvp4c* is included. The literature review is presented as well.

The second chapter deals with the review of an article by Bachok et al. [27]. It presents the boundary layer flow and heat transfer of a viscous fluid over a moving flat plate with variable fluid properties. The system of governing equations has been solved by the shooting technique. The influence of the parameters has been discussed graphically. The numerical results computed are being compared by the previous data in a tabular form.

In the third chapter, the steady two-dimensional MHD flow has been considered over a stretching sheet in the presence of a magnetic field. Special cases have been discussed to examine the MHD boundary layer flow and the heat transfer characteristics. The governing boundary layer PDEs are transformed into ODEs by means of similarity transformations. The velocity and temperature distributions are computed by an efficient numerical approach known as the shooting method along with the *bvp4c* as well. Various graphs have been plotted to examine the behaviour of the momentum and thermal boundary layers.

In the fourth chapter, the MHD boundary layer flow and heat transfer over a stretching sheet has been investigated. Three special cases namely, the constant fluid properties, the variable, and exponential fluid properties dependence on temperature are discussed. The variable viscosity fluid as a function of temperature has been studied for the MHD flow and the heat transfer analysis. The similarity transformation has been used to reduce PDEs into ODEs. Results are presented in graphical and tabular form. Tables have been shown for important parameters like the Nusselt number and results have been compared with the literature.

The fifth chapter is about the concluding remarks of the research work included in this thesis along with the future recommendations. The results drawn out in the present thesis have been discussed in this chapter. Some ideas related to the future is given and how to further this work can be extended is described as well. Moreover, some open problems for further study in this area of research are also included.

Contents

1	Introduction	2
1.1	Literature Review	2
1.2	Preliminaries and Basic Definitions	4
1.2.1	Fluid	4
1.2.2	Newton's Law of Viscosity	4
1.2.3	Kinematic Viscosity	4
1.2.4	Density	5
1.2.5	Shear Stress	5
1.2.6	Heat Flux	5
1.2.7	Specific Heat Capacity	6
1.2.8	Thermal Conductivity	6
1.2.9	Prandtl Number	6
1.2.10	Nusselt Number	7
1.2.11	Skin Friction Coefficient	7
1.2.12	Magnetohydrodynamics (MHD)	7
1.2.13	Stagnation Point Flow	8
1.2.14	Boundary Layer Flows	8
1.3	Governing Equations	9

1.3.1	Continuity Equation	9
1.3.2	Conservation of Momentum	9
1.3.3	Conservation of Energy	10
1.4	Numerical Methods	10
1.4.1	Shooting Method	10
1.4.2	bvp4c	12
2	Numerical Solution of Boundary Layer Flow and Heat Transfer with Variable Viscosity on a Moving Flat Plate in a Parallel Free Stream	13
2.1	Problem Formulation	14
2.2	Special Cases	16
2.2.1	Case A : Constant Fluid Properties	16
2.2.2	Case B: Variable Fluid Properties	17
2.3	Numerical Methods	18
2.4	Results and Discussions	18
3	Numerical Solution of MHD Boundary Layer Flow and Heat Transfer over a Stretching Sheet with Variable Fluid Properties	21
3.1	Introduction	22
3.2	Mathematical Formulation	22
3.3	Special Cases	24
3.3.1	Case A : Constant Fluid Properties	24
3.3.2	Case B: Variable Fluid Properties	25
3.3.3	Case C: Exponential Temperature Dependency	26
3.4	Numerical Methods	26
3.5	Results and Discussions	27
3.6	Concluding Remarks	35

4	Numerical Solution of MHD Boundary Layer Flow and Heat Transfer over a Non-Linear Stretching Sheet with Variable Fluid Properties	37
4.1	Introduction	38
4.2	Mathematical Formulation	38
4.3	Special Cases	40
4.3.1	Case A : Constant Fluid Properties	40
4.3.2	Case B: Variable Fluid Properties	41
4.3.3	Case C: Exponential Temperature Dependency	42
4.4	Numerical Methods	42
4.5	Results and Discussions	43
4.6	Concluding Remarks	53
5	Conclusions and Outlook	55
	Bibliography	57

List of Tables

2.1	Values of the reduced skin friction coefficient $-f''(0)$ and reduced temperature gradient $-\theta'(0)$ for $Pr_o = 1$ and 10 in both Cases A and B.	19
3.1	Comparison of values of $-f''(0)$ and $-\theta'(0)$ for the variation of different parameters for Case A.	28
3.2	Comparison of values of $-f''(0)$ and $-\theta'(0)$ with different values of M at $\epsilon=0.1$ for Case B.	29
3.3	Comparison of values of $-f''(0)$ and $-\theta'(0)$ with different values of ϵ at $Pr = 1$ for Case C.	29
3.4	Comparison of values of $-f''(0)$ and $-\theta'(0)$ with different Prandtl numbers at $M= \epsilon=0.1$ and $n=1$	30
4.1	Comparison of values of $-f''(0)$ and $-\theta'(0)$ for the variation of different parameters for Case A.	44
4.2	Values of skin friction coefficient $Re_x^{1/2}C_f$ and $Re_x^{-1/2}Nu_x$ when $Pr=1$ compared with previous data.	44
4.3	Comparison of $Re_x^{-1/2}Nu_x$ for $m = 0, n = 0, M = 0$, and for various Prandtl numbers to previously published data.	45
4.4	Comparison of values of $-f''(0)$ and $-\theta'(0)$ with different values of M at $\beta=1$ for Case B.	45
4.5	Comparison of values of $-f''(0)$ and $-\theta'(0)$ with different values of M and Prandtl number Pr at for Case C.	46

4.6	Comparison of values of $-f''(0)$ and $-\theta'(0)$ with different Prandtl numbers at $M=0.1$, and $n=1$	47
-----	---	----

List of Figures

1.1	Geometrical interpretation of a boundary layer flow [11].	8
2.1	Velocity profiles for different values of ϵ when $Pr_o = 1$ and $a=1$	20
2.2	Temperature profiles for different values of Pr_o when $\epsilon=0$ and $a=1$	20
3.1	Velocity profiles for different cases at $Pr = 0.7$, $n = 1$ and $M = \epsilon = 0.1$	31
3.2	Temperature profiles for different cases at $Pr = 0.7$, $n = 1$ and $M = \epsilon = 0.1$	31
3.3	Velocity profiles for different values of magnetic parameter M with $n = 1$, $\epsilon = 0.1$ and $Pr=0.7$	32
3.4	Temperature profiles for different values of magnetic parameter M with $n = 1$, $\epsilon = 0.1$ and $Pr=0.7$	32
3.5	Velocity profiles for different values of magnetic parameter M with $n = 2$, $\epsilon = 0.1$ and $Pr=1$	32
3.6	Temperature profiles for different values of magnetic parameter M with $n = 2$, $\epsilon = 0.1$ and $Pr=1$	32
3.7	velocity profiles for different values of magnetic parameter M with $n = 1$, $\epsilon = 0.5$ and $Pr=10$	33
3.8	Temperature profiles for different values of temperature index parameter n with $M = 0.1$, $\epsilon = 0.5$ and $Pr=10$	33
3.9	Velocity profiles for different values of n with $M = 5$, $\epsilon = 0.1$ and $Pr=1$	33
3.10	Temperature profiles for various values of n with $M = 5$, $\epsilon = 0.1$ and $Pr=1$	33
3.11	Velocity profiles for different values of Prandtl number Pr at $M=0.1$	34
3.12	Temperature profiles for different values of Prandtl number Pr at $M=0.1$	34

3.13	Velocity profiles for different values of Prandtl number Pr at $M=5$	34
3.14	Temperature profiles for different values of Prandtl number Pr at $M=5$	34
3.15	Velocity profiles for different values of ϵ with $M=0.1$, $n=1$ and $Pr=0.7$	35
3.16	Temperature profiles for various values of ϵ with $M=0.1$, $n=1$ and $Pr=0.7$	35
3.17	Velocity profiles for different values of ϵ with $M=0.5$, $n=1$ and $Pr=0.7$	35
3.18	Temperature profiles for different values of ϵ with $M=0.5$, $n=1$ and $Pr=0.7$	35
4.1	Velocity profile for different cases (A, B and C) at $Pr=0.7$, $n=1$ and $M, \epsilon=0.1$	49
4.2	Temperature profiles for different cases (A, B and C) at $Pr=0.7$, $n=1$ and $M, \epsilon=0.1$. .	49
4.3	Velocity profiles for different values of magnetic parameter M with $n=1$, $\beta=1$ and $Pr=0.7$.	49
4.4	Temperature profiles for different values of magnetic parameter M with $n=1$, $\beta=1$ and $Pr=0.7$	49
4.5	Velocity profiles for different values of magnetic parameter M with $n=1$, $\beta=1$ and $Pr=0.7$.	50
4.6	Temperature profiles for different values of magnetic parameter M with $n=1$, $\beta=1$ and $Pr=0.7$	50
4.7	Velocity profiles for different values of magnetic parameter M with $n=1$, $\beta=1$ and $Pr=0.7$.	50
4.8	Temperature profiles for different values of magnetic parameter M with $n=1$, $\beta=1$ and $Pr=0.7$	50
4.9	Velocity profiles for different values of parameter β with $n=1$, $M=0.5$ and $Pr=0.7$. . .	51
4.10	Temperature profiles for different values of parameter β with $n=1$, $M=0.5$ and $Pr=10$.	51
4.11	Temperature profiles for different values of parameter β with $n=1$, $M=0.5$ and $Pr=10$.	51
4.12	Temperature profiles for different values of parameter β with $n=1$, $M=0.5$ and $Pr=0.7$.	51
4.13	Velocity profiles for different values of parameter β with $n=1$, $M=0.5$ and $Pr=0.7$. . .	52
4.14	Temperature profiles for different values of temperature index parameter n with $M=0.1$, $m=1$ and $Pr=1$	52
4.15	Velocity profiles for different values of temperature index parameter n with $M=0.1$, $m=1$ and $Pr=10$	52

4.16	Temperature distribution for various values of temperature index parameter n with $M = 0.1$, $m = 1$ and $Pr=0.7$	52
4.17	Temperature profiles for different values of Pr at $M = 0.1$	53
4.18	Velocity profiles for different values of Pr at $M=0.1$	53
4.19	Temperature profiles for different values of Pr at $M = 0.5$	53
4.20	Velocity profiles for different values of Pr at $M = 0.5$	53

Chapter 1

Introduction

In this chapter, literature review and some basic definitions related to this research work will be presented. These includes boundary layer equations, some pertinent definitions in fluid mechanics, and explanation of numerical methods.

In Section 1, a literature review is presented. In Section 2, some basic concepts, definitions and terminologies of fluid mechanics are introduced which will be used throughout this dissertation. The governing equations of momentum and thermal boundary layer are discussed in Section 3. Explanation of numerical methods is presented in Section 4.

1.1 Literature Review

The study of flow of the boundary layer and the heat transfer on a moving flat plate and over a stretching sheet in the presence of a magnetohydrodynamics MHD with variable fluid properties of a viscous fluid is considered in the present work. Sakiadis [5] studied the incompressible flow of the boundary layer on a flat plate in a continuous motion. Different from Blasius [12], who considered flow over a fixed plate, Sakiadis [5] investigated the flow of a movable plate in a stationary ambient fluid. The boundary layer problem was first studied by Sakiadis [5] on continuous solid surfaces. Andersson and Aarseth [15] examined the effects of physical fluid properties depending on a temperature in the Sakiadis flow problem. Elbashbeshy and Bazid [6] considered the variable viscosity effects on heat transfer analysis

over a continuous stretching surface.

A numerical investigation of MHD boundary layer flow over a heated stretching sheet with variable viscosity was analyzed by Pantokratoras [3]. Bachok et al. [27] presented the influence of variable viscosity on the flow of the boundary layer and the transfer of heat from a flat plate in a continuous motion. Ali et al. [10] have investigated the effect of induced magnetic field over a vertical flat plate of the MHD mixed convection stagnation point flow of a viscous fluid. Recently, Agbaje et al. [31] analyzed the effects of MHD stagnation point flow and heat transfer towards a stretching sheet.

Magnetohydrodynamics (MHD) is the study of the magnetic properties of the fluid which is electrically conductive. A number of applications were found in the study of MHD conductive fluid, including various problems of astrophysics and geophysics. Mukhopadhyay et al. [29] presented some important investigations on the flow and heat transfer over a stretching sheet, including variable viscosity effects in different physical conditions. The heat transfer from a stretching sheet with variable surface temperature was presented by Afzal [26]. Pavlov [18] studied the MHD boundary layer flow and obtained an exact similarity solution of an electrically conducting fluid due to the stretching of a plane elastic surface in the presence of a uniform transverse magnetic field.

The flow field of a stretching wall with a power-law velocity variation was discussed by Ali [22]. Prasad et al. [19] investigated the effects of variable fluid properties on the hydromagnetic flow and heat transfer over a nonlinear stretching sheet. Andersson et al. [14] investigated the MHD flow of an electrically conducting power-law fluid over a stretching sheet in the presence of a uniform transverse magnetic field by using similarity transformation obtained an analytical solution of the magneto-hydro-magnetic flow using a similarity transformation for the velocity and temperature fields. The momentum boundary layer for a linear stretching sheet in the cooling fluids was studied by Crane [20], whereas Afzal and Varshney [25] described the power law stretching. Andersson and Dandapat [13] extended the Newtonian boundary layer flow problem obeying the power-law model considered by Crane [20].

In Chapters 2, 3 and 4 of this thesis, the constant fluid properties, the variable viscosity and exponential temperature dependency cases are discussed. In the current work, Chapter 2 includes the flow of the boundary layer on a flat plate moving with variable viscosity in

a parallel free stream. Chapters 3 and 4 deal with the properties of the constant and variable fluid of the MHD flow and heat transfer over a linear and nonlinear stretching surfaces, respectively. Conclusion is drawn in Chapter 5.

1.2 Preliminaries and Basic Definitions

1.2.1 Fluid

A fluid is a substance that deforms continuously under an applied shear stress, no matter how small that shear stress may be. The fluids flow easily and conform to the shape of their container.

The fluids are generally divided into two groups, namely, the liquids and the gases. A state of matter, such as liquid or gas, wherein the components of particles can move past each other and which can move, has no fixed shape and offers little resistance to external stress.

1.2.2 Newton's Law of Viscosity

The viscosity of a fluid is a measure of its resistance between layers. Fluid's viscosity depends on its temperature. The viscosity of a liquid decreases with an increasing temperature, but the viscosity of gases increase with the increasing temperature.

Newton's law of viscosity defines the relationship between the shear stress and the shear rate of a fluid subject to a mechanical stress. Mathematically we write

$$\tau = \mu \frac{du}{dy}.$$

which is known as Newton's law of viscosity. All fluids that obey Newton's law of viscosity are called Newtonian fluids.

1.2.3 Kinematic Viscosity

The kinematic viscosity is the ratio of dynamic viscosity and the density. Mathematically

$$\nu = \frac{\mu}{\rho}.$$

1.2.4 Density

The fluid density is defined as the mass per unit volume and it is expressed as

$$\rho = \frac{m}{V}.$$

The density is said to be uniform if it is identical at every point of the fluid.

1.2.5 Shear Stress

Shear stress is the force per unit area. Mathematically we write

$$\tau = \frac{F}{A},$$

where τ is the shear stress, F is the applied force, A is the cross sectional area. The friction force per unit area at the wall is called the wall shear stress. The wall shear stress, τ_w is defined as

$$\tau_w = \mu \left(\frac{\partial u}{\partial y} \right)_{y=0},$$

where μ is the dynamic viscosity, u is the flow velocity and y is normal to the wall.

1.2.6 Heat Flux

Heat flux is defined as the amount of heat transferred per unit area per unit time to or from a surface. Heat flux is the rate of thermal energy that passes through a surface. The induced heat flux always flows from the hot to the cold side.

If the flow is laminar, heat and temperature gradient are related by Fourier's law, which is written as,

$$\vec{q} = -k\vec{\nabla}T,$$

where the vector \vec{q} is the heat flux $\frac{W}{m^2}$, k is the thermal conductivity, T is the temperature.

1.2.7 Specific Heat Capacity

Specific heat capacity is the heat or thermal energy needed to increase the temperature of a unit quantity of a substance from a single unit. Specific heat capacity C_p is a property that indicates the amount of energy stored in a material per unit mass per unit of temperature. The specific heat is the ability to maintain a particular amount of heat. All conductors have a relatively low specific heat capacity, but non-conductors have a high value for the specific heat capacity. The SI unit is $\frac{J}{kgK}$.

1.2.8 Thermal Conductivity

The thermal conductivity is the property of a material that indicates its ability to conduct heat. The thermal conductivity of a substance is the heat flow rate per unit area of the cross section of the unit temperature gradient. SI unit of thermal conductivity is $\frac{W}{mK}$.

1.2.9 Prandtl Number

The Prandtl number Pr is a dimensionless parameter representing the ratio of diffusion of momentum to heat diffusion in a fluid. The Prandtl number is given as follows:

$$Pr = \frac{\nu}{\alpha} = \frac{\text{viscous diffusion rate}}{\text{thermal diffusion rate}} = \frac{\mu/\rho}{k/C_p\rho} = \frac{C_p\mu}{k}$$

The heat diffuses rapidly compared to the velocity when Pr is small. For small values of the Prandtl number $Pr \ll 1$ the thermal diffusivity dominates, whereas with large values $Pr \gg 1$ the viscous diffusivity dominates. The Prandtl number controls the relative thickness of the momentum and thermal boundary layers in the heat transfer problems.

The Prandtl number is a characteristic of the fluid only. The most common gases have similar values. The Prandtl number Pr for air at room temperature is 0.71. Liquids generally have a high Prandtl number, with values as high as 10^5 for some oils.

1.2.10 Nusselt Number

Nusselt number is the ratio of convection to transfer heat by conduction through the normal to the boundary. It is denoted by Nu :

$$Nu_L = \frac{\text{Convection heat transfer}}{\text{Conductive heat transfer}} = \frac{hL}{k},$$

where h is the convective heat transfer coefficient of the flow, L is the characteristic length, k is the thermal conductivity of the fluid. A Nusselt number having convection and conduction of similar magnitude close to one, is a characteristic of a laminar flow. A large Nusselt number means very efficient convection.

1.2.11 Skin Friction Coefficient

Skin friction occurs when a fluid flows over a solid surface. The fluid is in contact with the body surface, resulting in a frictional force exerted on the surface. The skin friction coefficient C_f is defined by:

$$C_f \equiv \frac{\tau_w}{\frac{1}{2}\rho U_\infty^2},$$

where τ_w is the local wall shear stress, ρ is the density of the fluid, and U_∞ is the free stream velocity. The dimensionless skin-friction is called the local skin-friction coefficient.

1.2.12 Magnetohydrodynamics (MHD)

Magnetohydrodynamics (MHD) is the study of the magnetic properties of electrically conductive fluids. Examples of such magneto-fluids include plasmas, liquid metals, and salt water or electrolytes. The fundamental concept behind MHD is that magnetic fields may induce currents in the conductive fluid in motion, which biases the fluid and reciprocally changes the magnetic field itself.

1.2.13 Stagnation Point Flow

In fluid dynamics, a stagnation point is a point in a flow field where the local fluid velocity is zero. Stagnation points exist at the surface of objects in the flow field, where the fluid is brought to rest by the object.

1.2.14 Boundary Layer Flows

A boundary layer is a layer of fluid in the immediate vicinity of a bounding surface where the viscosity effects are significant.

A boundary layer is formed by the thin region of flow adjacent to a surface, the layer in which the flow is influenced by the friction between the solid surface and the fluid. The analysis of the boundary layer helps to simplify the Navier-Stokes equations in order to solve these equations easily. In general, when a fluid flows past an object, the flow region can be divided into two parts. The larger part is related to a free stream of fluid i.e. outside the boundary layer where the viscous effects are not significant. In the thin region called boundary layer, where the effects of viscosity are important.

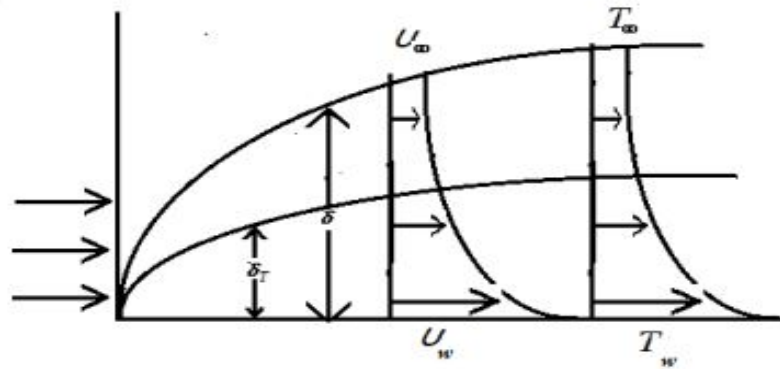


Figure 1.1: Geometrical interpretation of a boundary layer flow [11].

1.3 Governing Equations

The governing equations for fluid flow and heat transfer includes the continuity equation, the conservation of momentum, and the conservation of energy. Most of the fluid flow problems can be explained mathematically by these three equations.

1.3.1 Continuity Equation

The law of conservation of mass deals with the continuity equation.

$$\frac{\partial \rho}{\partial t} + \vec{\nabla} \cdot (\rho \vec{v}) = 0, \quad (1.3.1)$$

which is the equation of continuity for a compressible fluid. For steady flow

$$\frac{\partial \rho}{\partial t} = 0.$$

Then the above Eq. (1.3.1) becomes

$$\vec{\nabla} \cdot (\rho \vec{v}) = 0.$$

This is called a continuity equation or conservation equation of mass. If density $\rho = \text{constant}$ then we get

$$\vec{\nabla} \cdot \vec{v} = 0.$$

1.3.2 Conservation of Momentum

The conservation of momentum is based on the law of conservation of linear momentum.

$$\rho \left(\frac{d\vec{v}}{dt} \right) = -\vec{\nabla} \cdot \pi + \rho \vec{g}. \quad (1.3.2)$$

The surface forces occurred due to the stresses which are the summation of the viscous stresses τ_{ij} plus the hydrostatic pressure on the sides of control surface that comes from the motion of the velocity gradients. i.e.

$$\pi_{ij} = -p\delta_{ij} + \tau_{ij}.$$

So,

$$\vec{\nabla} \cdot \pi = -\vec{\nabla} p + \vec{\nabla} \cdot \tau.$$

Hence after substituting the above relation in equation (1.3.2), we get

$$\rho \left(\frac{d\vec{v}}{dt} \right) = -\vec{\nabla} p + \vec{\nabla} \cdot \tau + \rho \vec{g}. \quad (1.3.3)$$

1.3.3 Conservation of Energy

The conservation of energy is based on the first law of thermodynamics.

According to the first law of thermodynamics, the rate of change in energy equals the sum of the rate of heat addition to and work done on fluid particles.

$$\rho \frac{d\hat{U}}{dt} = -\vec{\nabla} \cdot \vec{q} - \vec{\nabla} \cdot (\pi \cdot \vec{v}) + (\vec{\nabla} \cdot \pi) \cdot \vec{v} \quad (1.3.4)$$

1.4 Numerical Methods

Numerical methods for ordinary differential equations (ODEs) are the methods used to find numerical approximations to the solutions of ODEs. To solve boundary value problems for the numerical study there exists some methods like, shooting method, *bvp4c* and finite difference method. In this dissertation, two numerical algorithms are used for the computational results, a shooting technique and a *bvp4c*, a built-in solver in MATLAB. The governing system of partial differential equations (PDEs) are transformed into an ordinary differential equations by means of similarity transformations. These numerical algorithms are explained below.

1.4.1 Shooting Method

In numerical analysis, the shooting method is a method for solving a boundary value problem BVP by reducing it to the solution of an initial value problem IVP. Shooting method can be used for both linear and non-linear ODEs. The basic algorithm of the shooting method is the supposition of trial value. The solution begins at one end of the boundary value problem and shoot to the other end with an initial value solver until the boundary condition at the other

end converges to its true value. The advantage of the shooting method is that the speed and adaptivity of initial value problems of methods are considered.

Consider the second order two point BVP subject to the boundary conditions that is written in the form as

$$y'' = f(x, y, y'), \quad y(a) = \alpha, \quad y(b) = \beta, \quad (1.4.1)$$

where (α, β) are unknowns.

The Eq. (1.4.1) is converted into IVP by the following procedure:

Consider the IVP

$$y'' = f(x, y, y'), \quad y(a) = \alpha, \quad y'(a) = \lambda. \quad (1.4.2)$$

Now from the above Eq. (1.4.2) we need to find the λ which will give the value of $y(b) = \beta$. The procedure for both the linear and nonlinear shooting method is similar to solve the IVPs except for few cases. The solution to nonlinear problems is same as linear problem except that the base solution cannot be expressed as a linear combination of each other. Moreover in a nonlinear case, we have an iterative procedure rather than a simple formula to combine the solutions of two IVPs. For a nonlinear BVP, we need to find a zero of the function representing the error i.e. the amount by which the solution to the IVP fails to satisfy the boundary condition at $x = b$. In other words the amount by which $y(b, \lambda)$ misses the target value β . This error is actually a function of the initial slope of our own choice so it is denoted as $F(\lambda)$. For different choices of λ , we get different errors, so we define

$$F(\lambda) = y(b, \lambda) - \beta = 0. \quad (1.4.3)$$

When $y'(a) = \lambda^*$ has been found then the desired solution is $y(x, \lambda^*)$.

Now two different approaches can be used to find the zero of the error function. One approach is we can use the secant method and the second approach is based on Newton's method. Here we described only the Newton's method.

In order to use Newton's method, we have to calculate the derivative of the function whose zero is required, namely, $F(\lambda)$. To choose the value of λ^* such that equation (1.4.3) holds. Then

$$\lambda^* = y'(a) = \frac{y(b) - y(a)}{b - a} \quad (1.4.4)$$

$$\lambda^* = \frac{\beta - \alpha}{b - a} \quad (1.4.5)$$

Newton's method is used to approximate the solution of $y(b, \lambda) - \beta = 0$ and find a next guess λ_{k+1} .

$$\lambda_{k+1} = \lambda_k - \frac{y'(b, \lambda_k) - \beta}{y'(b, \lambda_k)}. \quad (1.4.6)$$

1.4.2 `bvp4c`

To solve BVP directly we take help from `bvp4c`. Programming in MATLAB requires an estimate to solve BVP. The `bvp4c` is such an efficient solver to solve BVP's. `bvp4c` is based on collocation and solution begins with the initial estimate provided initial mesh points. As BVPs are much difficult to resolve in this respect, `bvp4c` is an efficient solver. Contrary to the shooting method, the solution is approximated on the entire interval and the boundary conditions are considered all times [21]. To represent the solution to the specified accuracy, the number of mesh points are needed as the cost of solving a BVP with `bvp4c` depends strongly on these numbers so, it tries to minimize this number.

Chapter 2

Numerical Solution of Boundary Layer Flow and Heat Transfer with Variable Viscosity on a Moving Flat Plate in a Parallel Free Stream

This chapter concerns with the boundary layer flow and heat transfer analysis along with variable fluid properties on a moving flat plate in a parallel free stream. It also includes the variation of fluid viscosity with temperature. This chapter is the literature review of Bachok et al. [27]. The boundary layer problem has been first studied by Sakiadis [5] on continuous solid surfaces. Pop et al. [16] and Andersson [15] have considered the boundary layer flow problems, including the variation of fluid viscosity with temperature. Bachok et al. [27] have considered the first case of steady boundary layer flow and heat transfer with variable fluid properties in a parallel free stream on a moving plate.

In this study, two special cases of constant fluid properties and variable fluid properties are discussed for boundary layer flow and heat transfer analysis. Numerical results obtained by using *bvp4c* and shooting method technique for various values of free stream parameter and the Prandtl number.

This chapter is organized as follows. Section 1 deals with the mathematical formulation, in

Section 2 special cases are discussed, Section 3 is about the details of numerical methods that we used for the numerical computations, Section 4 deals with results and discussions.

2.1 Problem Formulation

Consider a steady, two-dimensional boundary layer flow of a viscous fluid on a moving flat plate in a parallel free stream. Let the plate is moving with a constant velocity U_w and free stream velocity is U_0 . The moving plate is kept at constant temperature T_w and the ambient fluid has constant temperature T_0 .

Under the boundary layer assumptions, the equations governing the flow and heat transfer are given by Andersson and Aarseth [15],

$$\frac{\partial(\rho u)}{\partial x} + \frac{\partial(\rho v)}{\partial y} = 0, \quad (2.1.1)$$

$$\rho \left(u \frac{\partial u}{\partial x} + v \frac{\partial u}{\partial y} \right) = \frac{\partial}{\partial y} \left(\mu \frac{\partial u}{\partial y} \right), \quad (2.1.2)$$

$$\rho C_p \left(u \frac{\partial T}{\partial x} + v \frac{\partial T}{\partial y} \right) = \frac{\partial}{\partial y} \left(k \frac{\partial T}{\partial y} \right), \quad (2.1.3)$$

subject to the following boundary conditions

$$\begin{aligned} u = U_w, \quad v = 0, \quad T = T_w \quad \text{at} \quad y = 0, \\ u \rightarrow U_0, \quad T \rightarrow T_0 \quad \text{as} \quad y \rightarrow \infty. \end{aligned} \quad (2.1.4)$$

Here u and v denotes the components of velocity along the x and y directions respectively, T is the fluid temperature, C_p is the specific heat at constant temperature, ρ is the fluid density, μ is the dynamic viscosity and k is the thermal conductivity.

The following transformation is considered to examine the flow as mentioned in Andersson and Aarseth [15].

$$\eta = \sqrt{\frac{U}{a\nu_0 x}} \int \frac{\rho}{\rho_0} dy, \quad \psi = \rho_0 \sqrt{a\nu_0 x U} f(\eta), \quad (2.1.5)$$

$$\theta(\eta) = \frac{T - T_0}{T_w - T_0}, \quad (2.1.6)$$

where $U = U_w + U_0$, a is a dimensionless positive constant. Further ρ_0 , ν_0 , μ_0 , k_0 and C_{p_0} are the values of ambient fluid at temperature T_0 .

A stream function $\psi(x, y)$ is defined as

$$\rho u = \frac{\partial \psi}{\partial y}, \quad \rho v = -\frac{\partial \psi}{\partial x}. \quad (2.1.7)$$

And the velocity components are given as follows:

$$u = U f'(\eta), \quad v = \frac{\rho_0}{2} \sqrt{\frac{aU\nu_0}{x}} (\eta f'(\eta) - f), \quad (2.1.8)$$

By using the transformations given in Eqs. (2.1.5-2.1.8), the PDEs (2.1.1-2.1.3) can be transformed into the following ODEs

$$\frac{2}{a} \left(f'' \frac{\mu\rho}{\mu_0\rho_0} \right)' + f f'' = 0, \quad (2.1.9)$$

$$\left(\frac{k\rho}{k_0\rho_0} \theta' \right)' + \frac{C_p a}{2C_{p_0}} Pr_0 f \theta' = 0, \quad (2.1.10)$$

where Pr_0 is the constant Prandtl number of the ambient fluid. It can be expressed as:

$$Pr_0 = \mu_0 C_{p_0} / k_0.$$

The transformed boundary conditions (2.1.4) become

$$\begin{aligned} f(0) = 0, \quad f'(0) = 1 - \epsilon, \quad \theta(0) = 1, \\ f'(\eta) = \epsilon, \quad \theta(\eta) = 0 \quad \text{as } \eta \rightarrow \infty, \end{aligned} \quad (2.1.11)$$

where ϵ is the free stream parameter since it gives the relative importance of free stream velocity. It is defined as:

$$\epsilon = \frac{U_0}{U} = \frac{U_0}{U_0 + U_w}$$

The free stream parameter for different values correspond to different type of flows, such as a free stream velocity becomes equal to the moving plate velocity for $\epsilon=1/2$, for $\epsilon=1$ corresponds to the classical Blasius flow, and $\epsilon=0$ is for the case of a moving flat plate in a quiescent fluid (Sakiadis flow). For $0 < \epsilon < 1$, it corresponds to the case where both the velocities of free stream and plate are in the same direction.

While for $\epsilon > 1$, the free stream is directed towards positive x -axis while plate moves towards the negative x -axis. If $\epsilon < 0$, then the free stream is directed towards the negative x -axis while plate moves towards positive x -direction see Afzal et al. [26]. For our analysis, we consider only the case where the free stream is fixed and have positive-direction i.e. $\epsilon \geq 0$.

The surface shear stress τ_w and the surface heat flux q_w , which are defined as follows:

$$\tau_w = \mu_w \left(\sqrt{\frac{U^3}{a\nu_0 x}} f''(0) \right), \quad q_w = \mu_w C p_0 \Delta T P r_0^{-1} \sqrt{\frac{U}{a\nu_0 x}} [-\theta'(0)]. \quad (2.1.12)$$

2.2 Special Cases

2.2.1 Case A : Constant Fluid Properties

For Case A, the similarity variable η and stream function ψ simplifies to the Blasius [12] variable and are defined as

$$\eta = \sqrt{\frac{U}{a\nu_0 x}} y, \quad \psi = \sqrt{aU\nu_0 x} f(\eta). \quad (2.2.1)$$

Eqs. (2.1.9) and (2.1.10) reduce to

$$\frac{2}{a} f'''(\eta) + f f''(\eta) = 0, \quad (2.2.2)$$

$$\theta''(\eta) + \frac{a}{2}Pr_0 f(\eta)\theta'(\eta) = 0. \quad (2.2.3)$$

The case for $\epsilon=1$ was discussed by Fang [30], the Eq. (2.2.2) is an extended Blasius equation, where the solution of these equations is subjected to the same boundary conditions as given in Eq. (2.1.11).

2.2.2 Case B: Variable Fluid Properties

For Case B, we consider only the viscosity as a function of the temperature, while all the other fluid properties remained as constant.

$$\left(\frac{\mu}{\mu_0} f''\right)' + f(\eta) f''(\eta) - f'^2(\eta) = 0. \quad (2.2.4)$$

Pop et al. [16] and Andersson and Aarseth [15] followed the assumption that viscosity is an inverse linear function of temperature investigated by Lai and Kulacki [8] is given by the following equation;

$$\mu(T) \approx \frac{\mu_{ref}}{[1 + \gamma(T - T_0)]}, \quad (2.2.5)$$

here γ is a fluid property that depends on the reference temperature T_{ref} .

Generally viscosity has an inverse relation with temperature for liquids as with an increase in temperature the viscosity of liquids decreases ($\gamma > 0$), whereas for gases it increases ($\gamma < 0$).

If the reference temperature $T_{ref} \approx T_0$, the formula (2.2.5) can be expressed as

$$\mu = \frac{\mu_0}{1 - \frac{T - T_0}{\theta_{ref}(T_w - T_0)}}, \quad (2.2.6)$$

where θ_{ref} is defined as

$$\theta_{ref} = \frac{-1}{(T_w - T_0)\gamma},$$

which is a dimensionless constant and ΔT is the operating temperature difference ($T_w - T_0$).

Substituting the above formula (2.2.6) in Eq. (2.2.4) we get

$$f''' + \frac{\theta'}{\theta_{ref} - \theta} f'' + \frac{a}{2} \left(\frac{\theta_{ref} - \theta}{\theta_{ref}} \right) f f'' = 0. \quad (2.2.7)$$

The thermal energy boundary layer equation remains the same as in Eq. (2.2.3).

2.3 Numerical Methods

The numerical approach is used to find the numerical solutions of boundary layer problems. Numerical solutions of the governing equations are obtained by using the shooting method with fifth order Runge-Kutta integration method and MATLAB built-in solver *bvp4c*. The non-linear ordinary differential equations (ODEs) along with boundary conditions are solved by a numerical technique known as shooting method. The results are compared with those of *bvp4c*.

For Case A: The equation of momentum Eq. (2.2.2) becomes,

$$y_3' = -\frac{a}{2} y_1 y_3 \quad (2.3.1)$$

For Case B: The equation of momentum Eq. (2.2.7) becomes,

$$y_3' = \frac{y_3 y_5}{0.25 + y_4} - \frac{a y_1 y_3}{0.50} (0.25 + y_4). \quad (2.3.2)$$

While the thermal energy equation Eq. (2.2.3) remains the same for both the Cases A and B. The Eq. (2.2.3) becomes

$$y_5' = -\frac{a}{2} Pr_0 y_1 y_5. \quad (2.3.3)$$

2.4 Results and Discussions

In this section, numerical results are presented in tabular and graphical forms. The solution of boundary value problems of Eqs. (2.2.2-2.2.4) is a two-parameter problem that depends

on T_0 , Pr_0 and $(T_w - T_0)$, where the Prandtl number Pr_0 is related to T_0 . Bachok et al. [27] focus on the effects of a temperature dependent viscosity while assuming all other physical properties constant. Two different cases are observed to describe the effect of a temperature-dependent viscosity. Fluid is considered at temperature $T_0 = 278$ K as an ambient fluid and the temperature of the surface is $T_w = 358$ K where the operating temperature difference $\Delta T = T_w - T_0$ is 80 K at $Pr_0 = 10$ and 1. In Table 2.1 numerical results of skin friction coefficient $f''(0)$ and temperature gradient $\theta'(0)$ are obtained and compared with the results of Bachok et al. [27] by using *bvp4c* and shooting method. Comparison of results of constant fluid properties with the variable fluid properties at $Pr_0 = 10$ and 1 is shown and $\theta_{ref} = -0.25$ is set for water at $T_0 = 278$ K. For liquids, θ_{ref} is taken as negative and for the gasses it is taken as positive as mentioned in Ling and Dybbs [17].

Table 2.1: Values of the reduced skin friction coefficient $-f''(0)$ and reduced temperature gradient $-\theta'(0)$ for $Pr_o = 1$ and 10 in both Cases A and B.

ϵ	Pr_o	a	Bachok et al. [27]		Present results using <i>bvp4c</i>		Present results by shooting method	
			$-f''(0)$	$-\theta'(0)$	$-f''(0)$	$-\theta'(0)$	$-f''(0)$	$-\theta'(0)$
0	10	1						
Case A			0.4437	1.6803	0.4437	1.6802	0.4437	1.6803
Case B			1.3006	1.5292	1.3006	1.5292	1.3005	1.5292
0	1	1						
Case A			0.4437	0.4437	0.4437	0.4437	0.4437	0.4437
Case B			1.0381	0.3181	1.0381	0.3181	1.0381	0.3181

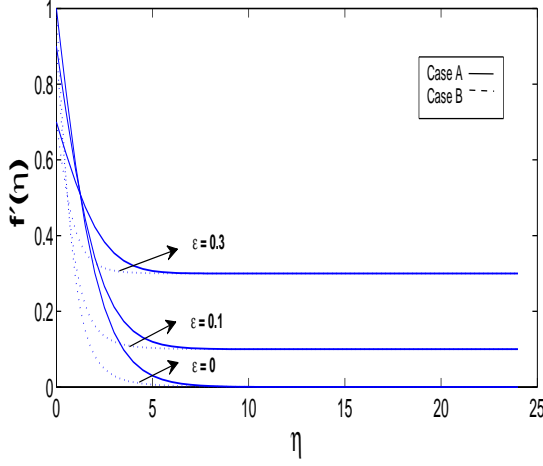


Figure 2.1: Velocity profiles for different values of ϵ when $Pr_o = 1$ and $a=1$.

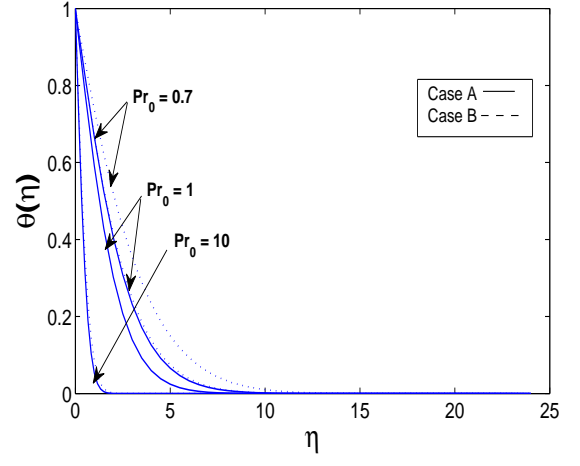


Figure 2.2: Temperature profiles for different values of Pr_o when $\epsilon=0$ and $a=1$.

The values of $f''(0)$ and $\theta'(0)$ are in very good correspondence with the results calculated by Andersson and Aarseth [15]. Therefore, this numerical approach can be used for the better approximation in order to validate the accuracy of the technique.

The reduced velocity profiles $f'(\eta)$ near the moving surface for Case B as compared with the case A is shown in Fig. (2.1). The moving surface heats the adjacent surface and reduces its viscosity. The temperature profile shows a higher temperature near the surface due to reduced viscosity for case B as shown in Fig. (2.2).

A necessary condition is analyzed by Andersson and Aarseth [15] that the integration length is sufficient long to satisfy $f''(0) \rightarrow 0$ and $\theta'(0) \rightarrow 0$ therefore the results obtained in Figs. (2.1) and (2.2) are produced at $\eta_0 = 25$. The momentum boundary layer and thermal boundary layer thickness decreases with an increase in the Prandtl number and free stream velocity. As compared to variable viscosity the constant fluid properties shows drag reduction characteristics.

Chapter 3

Numerical Solution of MHD Boundary Layer Flow and Heat Transfer over a Stretching Sheet with Variable Fluid Properties

This chapter is the extension work of Bachok et al. [27] presented in Chapter 2. In this chapter MHD boundary layer flow and heat transfer over a stretching sheet with variable fluid properties in a parallel free stream is investigated. The variation of viscosity on temperature is taken into account. The stretching sheet is moving with the non-uniform velocity. The stagnation point flow and heat transfer characteristics over a stretching sheet in the presence of a uniform magnetic field are studied.

Three special cases of constant fluid properties and variable fluid properties along with exponentially temperature dependence are discussed for boundary layer flow and heat transfer analysis. The effects of different parameters on the flow field and heat transfer characteristics are analyzed by using a shooting technique and *bvp4c*, a built-in solver in MATLAB.

This chapter is organized into different sections. Section 1 is related to introduction. Section 2 deals with the mathematical formulation. In Section 3 special cases are discussed. Section 4 is about the details of numerical methods that we used for the numerical computations.

Section 5 deals with results and discussions and Section 6 is about the conclusion.

3.1 Introduction

Magnetohydrodynamics (MHD) is the study of the magnetic properties of electrically conducting fluids. A number of applications have been found in the study of magnetohydrodynamics of a conducting fluid including various problems of astrophysics and geophysics. Makinde et al. [28] investigated the steady state mixed convection flow of a chemically reacting variable viscosity incompressible radiating and conducting fluid past a vertical porous convectively permeable plate in a porous medium in the presence of thermophoresis and a magnetic field. Lai and Kulacki [8] considered the effects of variable viscosity on convective heat transfer along a vertical surface in a porous medium. Ishak et al. [4] analyzed the unsteady MHD flow and heat transfer over a stretching plate and gave the numerical solution using similarity transformation technique. Bachok et al. [27] presented the influence of variable viscosity on boundary layer flow and heat transfer due to a continuously moving flat plate.

3.2 Mathematical Formulation

We consider a steady, two-dimensional magnetohydrodynamic laminar boundary layer flow of a viscous fluid near the stagnation point towards a stretching sheet. The velocity of the stretching surface $U_w(x) = ax$ and the free stream velocity $U_o(x) = bx$, are assumed to be linearly varying with x , distance from the stagnation point, where a and b are constants with $a > 0$ and $b > 0$. The uniform ambient fluid temperature is taken as T_o , while the temperature of the sheet is subjected to a prescribed temperature $T_w(x) = T_o + cx^n$, where c and n are constants with $c > 0$. A magnetic field of uniform strength B_o is applied along y -direction normal to the stretching sheet. All fluid properties are assumed to be constant

except for the viscosity which varies with temperature in the momentum equation. The governing equations for the MHD boundary layer flow and heat transfer of a steady laminar and compressible viscous fluid takes the form as:

$$\frac{\partial(\rho u)}{\partial x} + \frac{\partial(\rho v)}{\partial y} = 0, \quad (3.2.1)$$

$$\rho \left(u \frac{\partial u}{\partial x} + v \frac{\partial u}{\partial y} \right) = U_0 \frac{dU_0}{dx} + \frac{\partial}{\partial y} \left(\mu \frac{\partial u}{\partial y} \right) + \sigma B_0^2 (U_0 - u), \quad (3.2.2)$$

$$\rho C_p \left(u \frac{\partial T}{\partial x} + v \frac{\partial T}{\partial y} \right) = \frac{\partial}{\partial y} \left(k \frac{\partial T}{\partial y} \right), \quad (3.2.3)$$

where u and v are the velocities in x and y -directions, respectively. Further ρ , μ , k , C_p , T and B_0 is the fluid density, dynamic viscosity, thermal conductivity, specific heat, fluid temperature and an applied magnetic field strength, respectively.

The appropriate boundary conditions are written as

$$\begin{aligned} u = U_w(x) = ax, \quad v = 0, \quad T = T_w(x) = T_0 + cx^n \text{ at } y = 0, \\ u \rightarrow U_0(x) = bx, \quad T \rightarrow T_0 \text{ as } y \rightarrow \infty. \end{aligned} \quad (3.2.4)$$

The momentum and energy equations can be transformed into the ODEs by using the following similarity transformation [4]

$$\eta = \sqrt{\frac{a}{\nu_0}} \int \frac{\rho}{\rho_0} dy, \quad \psi = \rho_0 \sqrt{a \nu_0} x f(\eta), \quad \theta(\eta) = \frac{T - T_0}{T_w - T_0}, \quad (3.2.5)$$

where ρ_0 and ν_0 are the values of ambient fluid at temperature T_0 . ψ is the stream function defined as

$$\rho u = \frac{\partial \psi}{\partial y}, \quad \rho v = -\frac{\partial \psi}{\partial x}, \quad (3.2.6)$$

which satisfies the continuity equation Eq. (3.2.1) under condition (3.2.6) and the velocity components are given as follows:

$$u = ax f'(\eta), \quad v = -\rho_0 \sqrt{a \nu_0} f(\eta). \quad (3.2.7)$$

Substituting Eqs. (3.2.5), (3.2.6) and (3.2.7) into Eqs. (3.2.1), (3.2.2) and (3.2.3) the governing equation are obtained as;

$$\left(f'' \frac{\mu \rho}{\mu_0 \rho_0} \right)' + f f'' - f'^2 + M(\epsilon - f') + \epsilon^2 = 0, \quad (3.2.8)$$

$$\left(\frac{k\rho}{k_0\rho_0}\theta'\right)' - (nf'\theta - f\theta')Pr_0\frac{C_p}{C_{p0}} = 0, \quad (3.2.9)$$

with the boundary conditions transformed into the following form:

$$\begin{aligned} f(0) &= 0, \quad f'(0) = 1, \quad \theta(0) = 1, \\ f'(\eta) &= \epsilon, \quad \theta(\eta) = 0 \quad \text{as } \eta \rightarrow \infty, \end{aligned} \quad (3.2.10)$$

where f' and θ are the dimensionless velocity and temperature respectively. The other quantities are

$Pr_0 = \mu_0 C_{p0}/k_0$ is the Prandtl number

$M = \frac{\sigma B_0^2}{\rho a}$ is the magnetic parameter

$\epsilon = \frac{b}{a}$ is the velocity ratio parameter.

The surface shear stress τ_w and the surface heat flux q_w are the physical quantities of the main interest. These are defined as follows:

$$\tau_w = \mu_w \left(\frac{\partial u}{\partial y}\right) \Big|_{y=0}, \quad q_w = -k_w \frac{\partial T}{\partial y} \Big|_{y=0}, \quad (3.2.11)$$

Using Eq.(3.2.11) takes and take the following form:

$$\tau_w = \mu_w x \sqrt{\frac{a^3}{\nu_0}} f''(0), \quad q_w = \mu_w C_{p0} \Delta T Pr_0^{-1} \sqrt{\frac{a}{\nu_0}} [-\theta'(0)]. \quad (3.2.12)$$

3.3 Special Cases

3.3.1 Case A : Constant Fluid Properties

For Case A, the similarity variable η and stream function ψ reduces to the Blasius [12] variable

$$\eta = \sqrt{\frac{a}{\nu_0}} y, \quad \psi = \sqrt{a\nu_0} x f(\eta), \quad (3.3.1)$$

and Eqs. (3.2.8) and (3.2.9) reduce to

$$f''' + ff'' - f'^2 + M(\epsilon - f') + \epsilon^2 = 0, \quad (3.3.2)$$

$$\theta'' - (nf'\theta - f\theta')Pr_0 = 0. \quad (3.3.3)$$

These equations are subject to same boundary conditions given in Eq. (3.2.10) of Ishak et al. [4].

3.3.2 Case B: Variable Fluid Properties

In this case, we emphasize to study the variation of viscosity which varies with temperature while all the other fluid properties remained constant. Followed by Pop et al. [16], Andersson and Aarseth [15] and Elbashbeshy and Bazid [6] considered viscosity as a function of temperature and other properties as constant.

In this case the momentum boundary layer Eq. (3.2.8) becomes

$$(f'' \frac{\mu}{\mu_0})' + ff'' - f'^2 + M(\epsilon - f') + \epsilon^2 = 0. \quad (3.3.4)$$

For a viscous fluid, Bachok et al. [27] followed Ling and Dybbs [17] and assumed that the viscosity is an inverse linear function of temperature $\mu(T)$ proposed by Lai and Kulachi [8] given by the following equation

$$\mu(T) = \frac{\mu_{ref}}{[1 + \gamma(T - T_{ref})]}. \quad (3.3.5)$$

Here γ is a fluid property that depends on the reference temperature T_{ref} . If the reference temperature $T_{ref} \approx T_0$, the formula (15) can be written as follows

$$\mu = \frac{\mu_0}{1 - \frac{T-T_0}{\theta_{ref}(T_w-T_0)}} = \frac{\mu_0}{1 - \frac{\theta(\eta)}{\theta_{ref}}}. \quad (3.3.6)$$

where

$$\theta_{ref} \equiv \frac{-1}{(T_w-T_0)\gamma}$$

and $(T_w - T_0)$ is the operating temperature difference ΔT .

Using above formula (3.3.6) in Eq. (3.3.2) we get the momentum boundary equation for this case as

$$f''' = \frac{f''\theta'}{0.25 + \theta} - \frac{0.25 + \theta}{0.25} [ff'^2 - f'^2 - Mf' + \epsilon^2 + M\epsilon]. \quad (3.3.7)$$

3.3.3 Case C: Exponential Temperature Dependency

For Case C, the formula for the variation of the dynamic viscosity of the fluid with temperature is given by [9]

$$\ln\left(\frac{\mu}{\mu_{ref}}\right) \approx -2.10 - 4.45\frac{T_{ref}}{T} + 6.55\left(\frac{T_{ref}}{T}\right)^2, \quad (3.3.8)$$

and the momentum equation Eq. (3.3.4) after using above formula (3.3.8) for this case becomes,

$$f''' = (f'^2 - f f'' - \epsilon^2 - M\epsilon + M f')\left(\frac{\mu_0}{\mu}\right) - f''\theta'(T_w - T_0)\left(4.45\frac{T_{ref}}{T^2} - 13.1\frac{T_{ref}^2}{T^3}\right). \quad (3.3.9)$$

here

$\mu_{ref} = 0.00179$ kg/ms and $T_{ref} = 273$ K.

3.4 Numerical Methods

Numerical results are obtained by using shooting method. In shooting method, Newton-Raphson method has been used for root finding. The Runge-Kutta fifth order method has been utilized to find the solution of the reduced IVP. These results are verified by using MATLAB built-in solver *bvp4c*, which employs collocation technique in the background. To convert boundary value problems into an initial value problems we define new variables as,

$$\begin{aligned} y &= f = y_1, \\ f' &= y_1' = y_2, \\ f'' &= y_2' = y_3, \\ \theta &= y_4, \\ \theta' &= y_4' = y_5. \end{aligned}$$

The following strategy has been used to find solutions for the cases A, B, and C.

(a) For Case A: The equation of momentum (3.3.4) becomes,

$$y_3' = -y_1y_3 + My_2 - M\epsilon - \epsilon^2 + y_2^2 \quad (3.4.1)$$

$$y_5' = -Pr_0(y_1y_5 - ny_2y_4). \quad (3.4.2)$$

(b) For Case B: The equation of momentum (3.3.7) becomes,

$$y_3' = \frac{y_3y_5}{0.25 + y_4} - \frac{0.25 + y_4}{0.25}(y_2^2 + My_2 - y_1y_2^2 - \epsilon^2 - M\epsilon). \quad (3.4.3)$$

(c) For Case C: The equation of momentum (3.3.9) becomes,

$$y_3' = -y_1y_5(T_w - T_0)\left(4.45\frac{T_r}{T^2} - 13.1\frac{T_r^2}{T^3}\right) + \frac{\mu_0}{\mu}(y_2^2 + My_2 - y_1y_2^2 - \epsilon^2 - M\epsilon). \quad (3.4.4)$$

here

$$\frac{\mu}{\mu_0} = \frac{\mu_{ref}}{\mu_0} \exp\left(-2.10 - 4.45\left(\frac{T_{ref}}{T}\right) + 6.65\left(\frac{T_{ref}}{T}\right)^2\right). \quad (3.4.5)$$

3.5 Results and Discussions

In this section, the numerical results are depicted in tabular and graphical forms. The system of non-linear ODEs is solved numerically by using shooting technique along with Runge-Kutta fifth order integration technique. The resulting system of differential equations is then compared those results with MATLAB *bvp4c*. The computations are performed to study the effects of variation of magnetic parameter M , Prandtl number Pr , velocity ratio parameter ϵ , temperature index parameter n . The behaviour of skin friction coefficient $-f''(0)$ and temperature gradient $-\theta'(0)$ with the variation in physical parameters are shown in Tables (3.1-3.4). By increasing the values of Prandtl number Pr , the temperature index n , and velocity ratio parameter ϵ , the temperature gradient increases while having a decreasing effect on the skin friction coefficient for the variation of velocity ratio parameter and it shows no change for the Prandtl number and temperature index parameter as shown in Tables 3.1

and 3.3. The influence of the variation of magnetic parameter has an increasing effect on the skin friction coefficient but there is a decrease in the temperature gradient for case A and case B as shown in Tables 3.1 and 3.2. Comparison of three cases have been depicted in Table 3.4 where the skin friction coefficient decreases for Case A and C as compared to case B and the temperature gradient increases for all cases with an increase of the Prandtl number.

Table 3.1: Comparison of values of $-f''(0)$ and $-\theta'(0)$ for the variation of different parameters for Case A.

Pr	M	ϵ	n	$bvp4c$		shooting method	
				$-f''(0)$	$-\theta'(0)$	$-f''(0)$	$-\theta'(0)$
0.7	0.1	0.1	1	1.0098928	0.81215822	1.0098933	0.81215098
1	-	-	-	1.0098928	1.0127478	1.0098933	1.0127415
3	-	-	-	1.0098928	1.9267086	1.0098933	1.9268326
7	-	-	-	1.0098928	3.0726765	1.0098933	3.0727008
10	-	-	-	1.0098928	3.7204164	1.0098933	3.7204954
0.7	0.2	-	-	1.0489058	0.80470808	1.048906	0.80470549
-	0.3	-	-	1.0865699	0.79764357	1.0865705	0.79764053
-	0.4	-	-	1.1230104	0.79092717	1.1230112	0.79092368
-	0.5	-	-	1.1583345	0.78452983	1.1583357	0.78452608
10	0.5	0.5	0	0.75401486	2.3769594	0.75401494	2.3769408
-	-	-	1	0.75401485	3.7947678	0.75401495	3.7947635
-	-	-	2	0.75401485	4.8705287	0.75401495	4.8705389
-	-	-	3	0.75401485	5.7661056	0.75401495	5.7661056
-	-	-	4	0.75401485	6.5476536	0.75401495	6.5476536
1	0.1	0.1	1	1.0098928	1.0127478	1.0098933	1.0127415
-	-	0.2	-	0.95185881	1.0396127	0.95185917	1.0396145
-	-	0.3	-	0.87735782	1.0669778	0.87735595	1.0669733
-	-	0.4	-	0.78812365	1.0944243	0.78812105	1.0944921
-	-	0.5	-	0.68543881	1.1217327	0.68543828	1.1217059

Table 3.2: Comparison of values of $-f''(0)$ and $-\theta'(0)$ with different values of M at $\epsilon=0.1$ for Case B.

				<i>bvp4c</i>		shooting method	
M	Pr	ϵ	n	$-f''(0)$	$-\theta'(0)$	$-f''(0)$	$-\theta'(0)$
0.1	1	0.1	1	1.9676843	0.9682156	1.9663873	0.9681393
0.2	-	-	-	2.0233129	0.9363979	2.0234264	0.9367586
0.3	-	-	-	2.1398691	0.9104215	2.1389705	0.9103190
0.4	-	-	-	2.2461303	0.8878961	2.2457508	0.8876009
0.5	-	-	-	2.3446827	0.8694642	2.3445932	0.8693543

Table 3.3: Comparison of values of $-f''(0)$ and $-\theta'(0)$ with different values of ϵ at Pr = 1 for Case C.

				<i>bvp4c</i>		shooting method	
ϵ	n	M	Pr	$-f''(0)$	$-\theta'(0)$	$-f''(0)$	$-\theta'(0)$
0.1	1	5	1	2.1441991	0.8317945	2.1441586	0.8317140
0.2	-	-	-	1.9202611	0.9134659	1.9202279	0.9134622
0.3	-	-	-	1.6885735	0.9783565	1.6885469	0.9783545
0.4	-	-	-	1.4486799	1.0345052	1.4486621	1.0345038
0.5	-	-	-	1.1995993	1.0860253	1.1970435	1.0842147

Table 3.4: Comparison of values of $-f''(0)$ and $-\theta'(0)$ with different Prandtl numbers at $M= \epsilon=0.1$ and $n=1$.

			<i>bvp4c</i>		shooting method	
Cases	ϵ	Pr	$-f''(0)$	$-\theta'(0)$	$-f''(0)$	$-\theta'(0)$
	0.1	0.7				
CaseA			1.0098928	0.81215822	1.0098933	0.81215098
CaseB			1.8661448	0.77697376	1.8661449	0.77697370
CaseC			1.0207258	0.9304605	1.0207252	0.93046040
	0.1	1				
CaseA			1.0098928	1.0127478	1.0098933	1.0127415
CaseB			1.9799072	0.86476828	1.9799070	0.86476819
CaseC			0.7253066	1.1012004	0.7253043	1.1012091
	0.1	10				
CaseA			1.0098928	3.7204164	1.0098933	3.7204964
CaseB			2.8841258	3.3669161	2.8841248	3.3669159
CaseC			0.7217002	3.8027996	0.7217190	3.8027980

Three cases have been considered to illustrate the effect of temperature-dependent viscosity. The surface temperature is taken as $T_w = 358\text{K}$. The ambient fluid is considered at temperature $T_0 = 278\text{K}$. Figs. 3.1 and 3.2 show the velocity and temperature profiles for three different cases A, B, and C. The temperature profile shows the reduction in Case C near the moving surface as compared to the other two cases A and B in Fig.3.2.

The influence of magnetic parameter M on velocity and temperature profiles is shown in Figs. 3.3-3.7. The presence of a magnetic field to an electrically conducting fluid give rise to a resistive force called the Lorentz force. This force can slow down the motion of the fluid. As the values of magnetic parameter M increases, Lorentz force increases and as a result the motion of the fluid decreases and the thickness of momentum boundary layer decreases. The increase in M causes an increase in the thickness of thermal boundary layer while decreases the thickness of momentum boundary layer for all cases. Figs. 3.8-3.10 shows the reduction in the thickness of thermal boundary layer due to an increase in temperature index parameter n and an increasing effect is shown for the velocity profile for case B.

The Prandtl number is the ratio of viscous diffusivity to the thermal diffusivity. Raising Prandtl number depicts the decrease in thermal boundary layer thickness while shows no change in the momentum boundary layer. The effect of Prandtl number on temperature profile which decreases with the increase in Prandtl number in Fig. 3.12 but the increase in Prandtl number has no such effect on velocity profile, at different values for Pr it gives the same result for case A , as shown in Fig. 3.11. While in Figs. 3.13-3.14 for case B there is an increase in the thickness of momentum boundary layer and decrease in the thermal boundary layer thickness with an increase in Prandtl number. The effect of variation of ϵ parameter is shown in Figs. 3.15-3.18, for case C and case A. The velocity profile increases, while the temperature profile decreases with an increase in the free stream parameter.

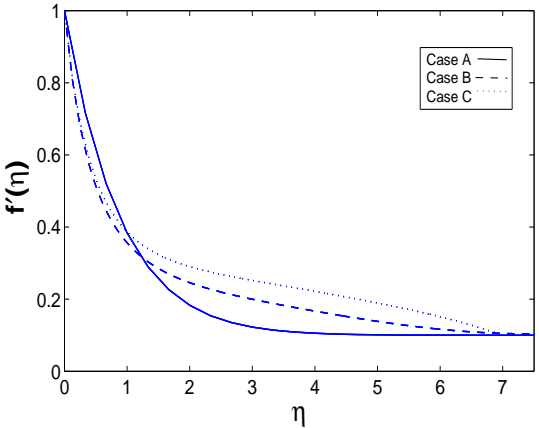


Figure 3.1: Velocity profiles for different cases at $Pr = 0.7$, $n = 1$ and $M = \epsilon = 0.1$.

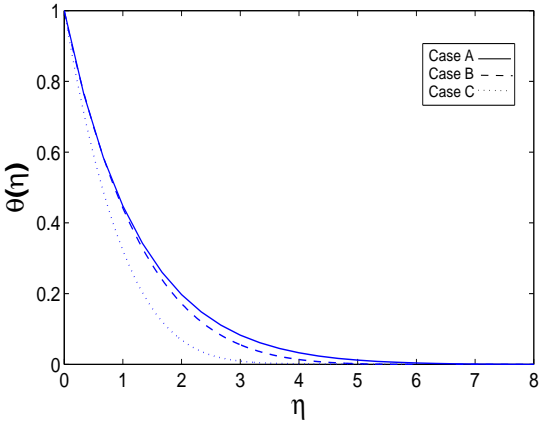


Figure 3.2: Temperature profiles for different cases at $Pr = 0.7$, $n = 1$ and $M = \epsilon = 0.1$.

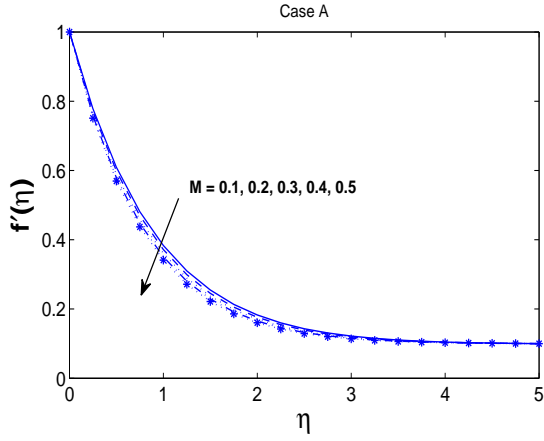


Figure 3.3: Velocity profiles for different values of magnetic parameter M with $n = 1$, $\epsilon = 0.1$ and $Pr=0.7$.

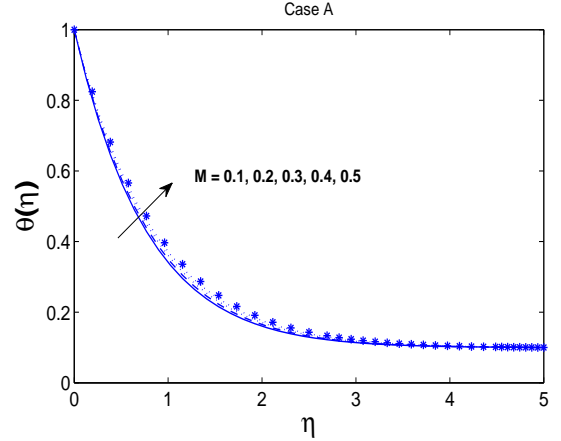


Figure 3.4: Temperature profiles for different values of magnetic parameter M with $n = 1$, $\epsilon = 0.1$ and $Pr=0.7$.

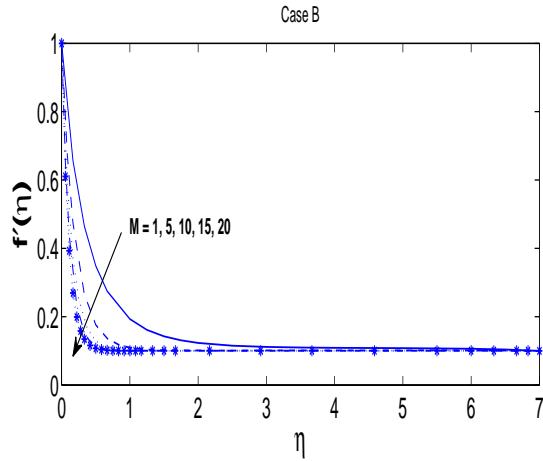


Figure 3.5: Velocity profiles for different values of magnetic parameter M with $n = 2$, $\epsilon = 0.1$ and $Pr=1$.

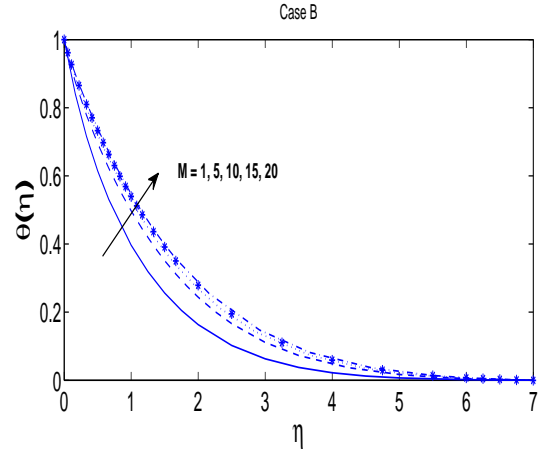


Figure 3.6: Temperature profiles for different values of magnetic parameter M with $n = 2$, $\epsilon = 0.1$ and $Pr=1$.

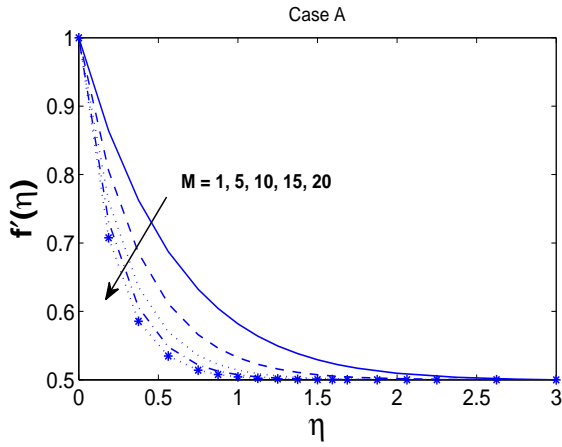


Figure 3.7: velocity profiles for different values of magnetic parameter M with $n = 1$, $\epsilon = 0.5$ and $Pr=10$.

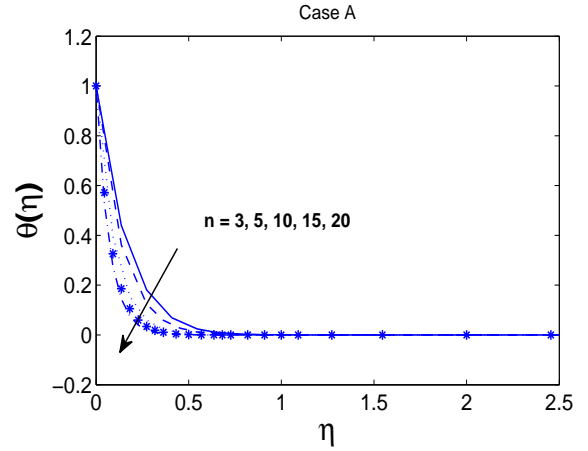


Figure 3.8: Temperature profiles for different values of temperature index parameter n with $M = 0.1$, $\epsilon = 0.5$ and $Pr=10$.

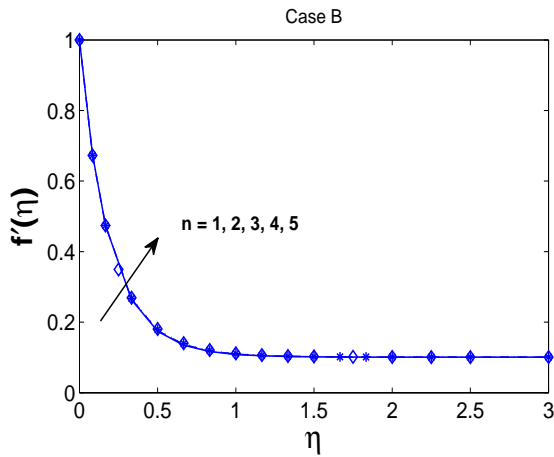


Figure 3.9: Velocity profiles for different values of n with $M = 5$, $\epsilon = 0.1$ and $Pr=1$.

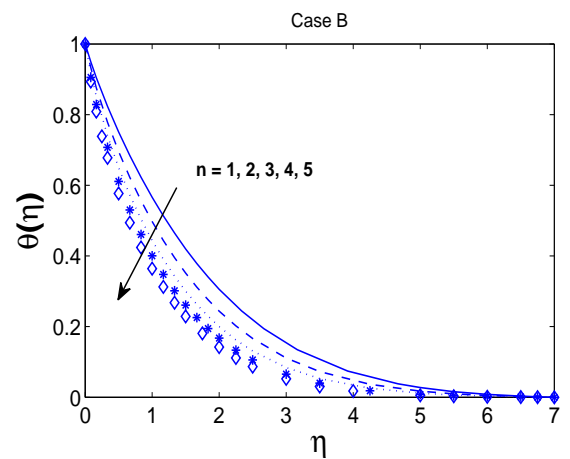


Figure 3.10: Temperature profiles for various values of n with $M = 5$, $\epsilon = 0.1$ and $Pr=1$.

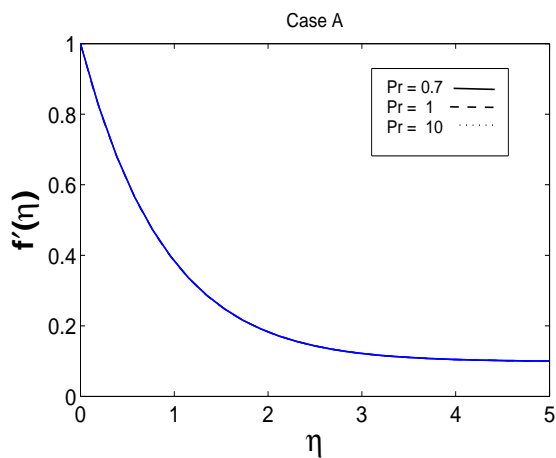


Figure 3.11: Velocity profiles for different values of Prandtl number Pr at $M=0.1$.

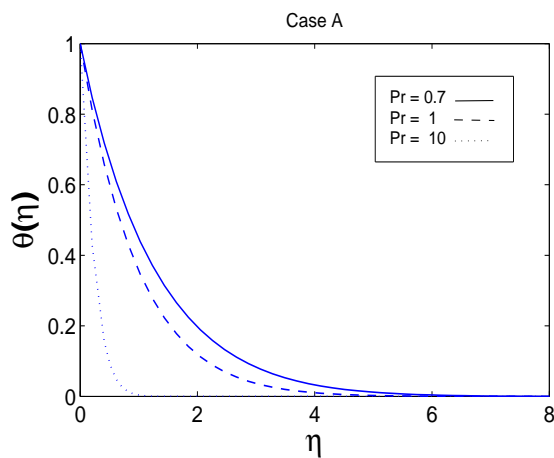


Figure 3.12: Temperature profiles for different values of Prandtl number Pr at $M=0.1$.

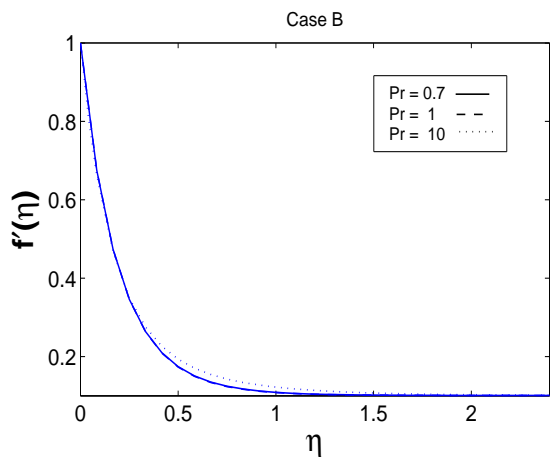


Figure 3.13: Velocity profiles for different values of Prandtl number Pr at $M=5$.

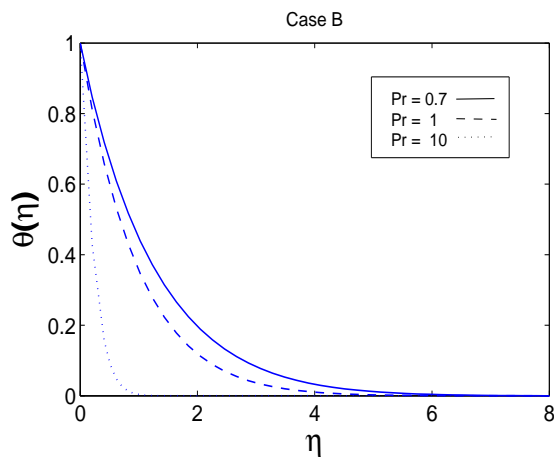


Figure 3.14: Temperature profiles for different values of Prandtl number Pr at $M=5$.

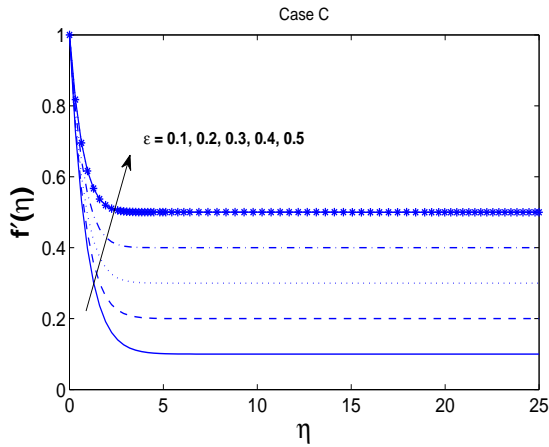


Figure 3.15: Velocity profiles for different values of ϵ with $M=0.1$, $n=1$ and $Pr=0.7$.

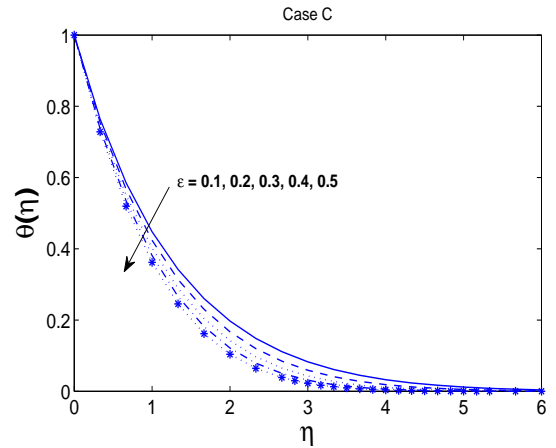


Figure 3.16: Temperature profiles for various values of ϵ with $M=0.1$, $n=1$ and $Pr=0.7$.

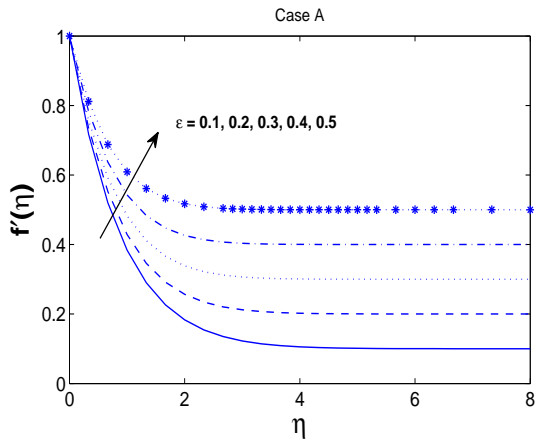


Figure 3.17: Velocity profiles for different values of ϵ with $M=0.5$, $n=1$ and $Pr=0.7$.

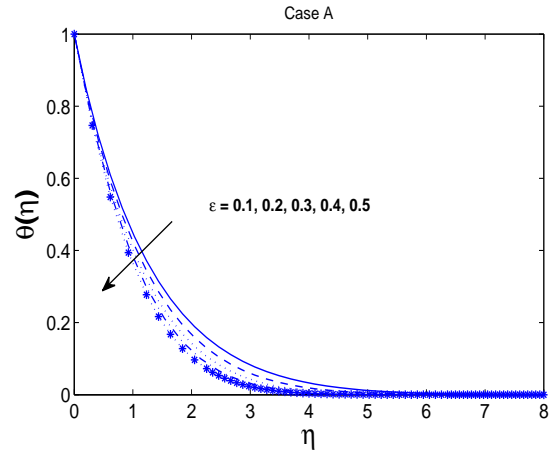


Figure 3.18: Temperature profiles for different values of ϵ with $M=0.5$, $n=1$ and $Pr=0.7$.

3.6 Concluding Remarks

The increase in MHD parameter resulted in an increase in the skin friction coefficient and in the thermal boundary layer thickness while decreases the thickness of momentum boundary layer as well as the wall temperature. The velocity ratio parameter ϵ caused an increasing effect in the thickness of momentum boundary layer and in the temperature gradient and reduced the thickness of the thermal boundary layer and the skin friction coefficient. It

is observed, the thermal boundary layer thickness decreases for all cases but the thickness of momentum boundary layer increases for case B and shows no effect for case A with an increase in the values of the Prandtl number while both the skin friction coefficient and the temperature gradient increases. The increase in temperature index parameter n resulted in an increase in the thickness of momentum boundary layer and the wall temperature while shows the opposite result for the skin friction coefficient and thermal boundary layer thickness.

Chapter 4

Numerical Solution of MHD Boundary Layer Flow and Heat Transfer over a Non-Linear Stretching Sheet with Variable Fluid Properties

The steady two-dimensional MHD boundary layer flow and heat transfer for a viscous fluid over a nonlinear stretching sheet with variable fluid properties is investigated. Three cases of constant fluid properties, variable temperature-dependency and exponentially temperature-dependency on the MHD boundary layer flow and heat transfer over a nonlinear stretching sheet have been investigated. The case of fluid viscosity vary as an inverse function and linear function of temperature is studied. The effect of various governing parameters on the velocity and temperature profiles and heat transfer characteristics are studied such as Prandtl number Pr , velocity exponent m , temperature index parameter n , the magnetic parameter M , and the stretching parameter β .

The governing nonlinear partial differential equations are transformed into non-linear ordinary differential equations by using the similarity transformation and are solved numerically by the shooting technique and *bvp4c*, a built-in solver of MATLAB. The numerical results for the velocity, temperature, skin friction coefficient, and the Nusselt number are obtained

and presented graphically and in tabular form for different values of the parameters.

4.1 Introduction

The current study pursues the work by Andersson and Aarsaeth [15]. In this work we study MHD boundary layer flow and heat transfer over a non-linear stretching sheet with variable fluid properties. Therefore to predict the flow and heat transfer rates, the variable fluid properties are taken into account. In view of this, the problem studied here extends the work of Andersson and Aarseth by considering the temperature-dependent variable fluid properties. The present work deals with numerical solutions for specific values of stretching parameter and the Prandtl number of flow behaviour and heat transfer characteristics. The coupled nonlinear partial differential equations governing the problem are transformed to a system of coupled nonlinear ordinary differential equations by applying a suitable similarity transformation. These non-linear coupled differential equations are solved numerically by the shooting method and *bvp4c*, a built-in solver of MATLAB for different values of the physical parameters.

This paper is organized as follows. In Section 2 we present model and mathematical formulation. Special cases are discussed in Section 3. Section 4 is related to the details of the numerical solution. Results and discussions are presented in Section 5 and Section 6 deals with the conclusion.

4.2 Mathematical Formulation

Consider a steady, two-dimensional magnetohydrodynamic (MHD) laminar boundary layer flow of a viscous fluid over a nonlinear stretching sheet in the presence of a transverse magnetic field. The sheet is moving with a non-uniform velocity $U(x)$ in an ambient fluid at rest. The stretching velocity of the sheet is of the form $U_w(x) = ax^m$, where a is a positive constant and m is an exponent. The ambient temperature of the fluid is taken as T_0 while the temperature of the sheet is subjected to a form $T_w(x) = T_0 + cx^n$ with $c > 0$, where c and n

behaves as a constant. Along the normal to the stretching sheet, a uniform magnetic field of strength B_0 is applied. The viscous dissipation and the induced magnetic field produced by an electrically conducting fluid are negligible. The laminar boundary layer equations for continuity, momentum and thermal energy for MHD flow are written as follows:

$$\frac{\partial(\rho u)}{\partial x} + \frac{\partial(\rho v)}{\partial y} = 0, \quad (4.2.1)$$

$$\rho \left(u \frac{\partial u}{\partial x} + v \frac{\partial u}{\partial y} \right) = \frac{\partial}{\partial y} \left(\mu \frac{\partial u}{\partial y} \right) - \sigma B_0^2 u, \quad (4.2.2)$$

$$\rho C_p \left(u \frac{\partial T}{\partial x} + v \frac{\partial T}{\partial y} \right) = \frac{\partial}{\partial y} \left(k \frac{\partial T}{\partial y} \right), \quad (4.2.3)$$

with corresponding boundary conditions,

$$u = U_w(x) = ax^m, \quad v = 0, \quad T = T_w(x) = T_0 + cx^n \text{ at } y = 0, \quad (4.2.4)$$

$$u \rightarrow 0, \quad T \rightarrow T_0 \text{ as } y \rightarrow \infty.$$

where u and v are the fluid velocities, ρ is the density of fluid, B_0 is an applied magnetic field strength. μ is the dynamic viscosity, C_p is the specific heat, T is the fluid temperature and k is the thermal conductivity of the fluid. U_w is the velocity at the sheet, T_w is the wall temperature.

We introduce the following dimensionless variables mentioned in Ali [23].

$$\eta = \sqrt{\frac{(1+m)U(x)}{2\nu x}} \int \frac{\rho}{\rho_0} dy, \quad \psi = \rho_0 \sqrt{\frac{2\nu x U(x)}{1+m}} f(\eta), \quad \theta(\eta) = \frac{T - T_0}{T_w - T_0}. \quad (4.2.5)$$

And ψ is the stream function defined as:

$$\rho u = \frac{\partial \psi}{\partial y}, \quad \rho v = -\frac{\partial \psi}{\partial x} \quad (4.2.6)$$

The relation of stream function ψ is introduced here to evaluate the velocity components, which are given as,

$$u = ax^m f'(\eta), \quad v = -\rho_0 \sqrt{\frac{2\nu a}{1+m}} x^{\frac{m-1}{2}} \left(\frac{m+1}{2} f(\eta) + \eta \frac{m-1}{2} f'(\eta) \right), \quad (4.2.7)$$

The following dimensionless quantities are introduced into the governing momentum and thermal energy equations,

$Pr = \mu C_p / k$ is the Prandtl number

$M = \frac{2\sigma B_0^2}{\rho a(1+m)x^{m-1}}$ is the magnetic parameter

$\beta = \frac{2m}{1+m}$ is the velocity ratio parameter.

By using Eqs. (4.2.5-4.2.7) into Eqs. (4.2.1-4.2.3) we get,

$$\left(f'' \frac{\mu\rho}{\mu_0\rho_0}\right)' + ff'' - \beta f'^2 - Mf' = 0, \quad (4.2.8)$$

$$\left(\frac{k\rho}{k_0\rho_0}\theta'\right)' + Pr(f\theta' - \frac{2n}{1+m}f'\theta) = 0, \quad (4.2.9)$$

and the boundary conditions becomes,

$$\begin{aligned} f(0) &= 0, & f'(0) &= 1, & \theta(0) &= 1, \\ f'(\eta) &= 0, & \theta(\eta) &= 0 & \text{as } \eta &\rightarrow \infty, \end{aligned} \quad (4.2.10)$$

here f' is the dimensionless velocity and θ is the dimensionless temperature.

The physical quantities of main interest are the surface shear stress τ_w and the surface heat flux q_w , which are defined as follows:

$$\tau_w = \mu_w x^{\frac{m+1}{2}} y \sqrt{\frac{a^3(1+m)}{2\nu}} f''(0), \quad q_w = \mu_w C_p \Delta T Pr^{-1} \sqrt{\frac{a(1+m)}{2\nu}} [-\theta'(0)]. \quad (4.2.11)$$

4.3 Special Cases

4.3.1 Case A : Constant Fluid Properties

We have taken all the fluid properties to be constant except the viscosity variation with temperature. In the first case, fluid properties are treated as constant. For Case A, the dimensionless variables η and stream function ψ reduces to a form

$$\eta = \sqrt{\frac{a}{\nu_0}} y, \quad \psi = \sqrt{a\nu_0} x f(\eta), \quad (4.3.1)$$

and Eqs. (4.2.8) and (4.2.9) under the above similarity transformation reduces to,

$$f''' + f f'' - \beta f'^2 - M f' = 0, \quad (4.3.2)$$

$$\theta'' + Pr(f\theta' - \frac{2n}{1+m}f'\theta) = 0, \quad (4.3.3)$$

along with the same boundary conditions given in Eq. (10). of Prasad et al. [19]. It should be noted here that by setting $M = 0$ in Eqs.(4.3.2) and (4.3.3) one can get a form of Eqs. (7-8) of N. Afzal [26] and Eqs. (14-17) of Prasad et al. [19] but here these set of equations are in simplest form.

4.3.2 Case B: Variable Fluid Properties

In the second case, we consider only the viscosity variation with temperature while taking all other fluid properties as constant. For Case B, variable fluid properties are considered. This is done by following Andersson and Aarseth [15], Elbashbeshy and Bazid [6] and Bachok et al. [27].

The momentum boundary layer Eq. (4.2.8) for this case becomes

$$(f'' \frac{\mu}{\mu_0})' + f f'' - \beta f'^2 - M f' = 0. \quad (4.3.4)$$

For a viscous fluid, the formula for the inversely linear temperature-dependence proposed by the following Lai and Kulachi [8], Ling and Dybbs [17] and Pop et al. [16] is given by the following equation

$$\mu(T) = \frac{\mu_{ref}}{[1 + \gamma(T - T_{ref})]}. \quad (4.3.5)$$

Here γ is a fluid property that depends on the reference temperature T_{ref} . Under the condition that if the reference temperature $T_{ref} \approx T_0$, the above formula (4.3.5) can be written as follows

$$\mu = \frac{\mu_0}{1 - \frac{T-T_0}{\theta_{ref}(T_w-T_0)}} = \frac{\mu_0}{1 - \frac{\theta(\eta)}{\theta_{ref}}}, \quad (4.3.6)$$

where $\theta_{ref} \equiv \frac{-1}{(T_w-T_0)\gamma}$ and $(T_w - T_0)$ is the operating temperature difference ΔT .

By substituting the formula (4.3.6) in Eq. (4.3.4), the following equation becomes

$$f''' + \frac{\theta'}{\theta_{ref} - \theta} f'' + (\frac{\theta_{ref} - \theta}{\theta_{ref}})(f f'' - M f' - \beta f'^2) = 0. \quad (4.3.7)$$

4.3.3 Case C: Exponential Temperature Dependency

For Case C, the formula for the variation of the dynamic viscosity of the fluid with temperature was recommended by [9]

$$\ln\left(\frac{\mu}{\mu_{ref}}\right) \approx -2.10 - 4.45\frac{T_{ref}}{T} + 6.55\left(\frac{T_{ref}}{T}\right)^2, \quad (4.3.8)$$

and the momentum boundary equation for Case C after substituting the above formula (4.3.8) becomes

$$f''' = -f''\theta'cx^n\left(4.45\frac{T_{ref}}{T^2} - 13.1\frac{T_{ref}^2}{T^3}\right) + \frac{\mu_0}{\mu}(\beta f'^2 - ff'' + Mf'). \quad (4.3.9)$$

4.4 Numerical Methods

The non-linear ordinary differential equations (ODEs) along with boundary conditions are solved numerically by the shooting technique. Newton Raphson method has been used for root finding. To find the solution of the reduced IVP, the Runge-Kutta fifth order method has been utilized. These computed results were verified by using MATLAB built-in solver *bvp4c*. By using the following strategy the momentum equation for Case A becomes,

(a) For case A:

$$y_3' = -y_1y_3 + \beta y_2^2 + My_2, \quad (4.4.1)$$

$$y_5' = Pr\left(\frac{2n}{1+m}y_2y_4 - y_1y_5\right) = 0. \quad (4.4.2)$$

(b) For case B: The equation of momentum becomes,

$$y_3' = \frac{y_3y_5}{0.25 + y_4} - \frac{0.25 + y_4}{0.25}(\beta y_2^2 + My_2 - y_1y_3). \quad (4.4.3)$$

(c) For case C: The equation of momentum becomes,

$$y_3' = -y_3y_5cx^n\left(4.45\frac{T_{ref}}{T^2} - 13.1\frac{T_{ref}^2}{T^3}\right) + \frac{\mu_0}{\mu}(\beta y_2^2 + My_2 - y_1y_3). \quad (4.4.4)$$

here

$$\frac{\mu}{\mu_0} = \frac{\mu_{ref}}{\mu_0} \exp\left(-2.10 - 4.45\left(\frac{T_{ref}}{T}\right) + 6.65\left(\frac{T_{ref}}{T}\right)^2\right). \quad (4.4.5)$$

$\mu_{ref} = 0.001792$ kg/ms, $\mu_0 = 0.001520$ kg/ms and $T_{ref} = 273\text{K}$, $T_0 = 278\text{K}$.

4.5 Results and Discussions

In this section, the numerical results obtained for the dimensionless velocity and temperature profiles for the variation of different physical parameters magnetic parameter M , velocity exponent m , stretching parameter β , temperature index parameter n are presented in tabular and graphical forms. The behaviour of skin friction coefficient $-f''(0)$ and temperature gradient $-\theta'(0)$ with the variation in physical parameters is shown in Tables (4.1-4.6). In Tables 4.2 and 4.3 the results are obtained for the Nusselt number and verified with the previous results obtained by Mustafa [24] and Ali [23] and in Tables 4.1 and 4.5, results are computed for the various values of Prandtl numbers Pr 0.72, 1, 3, and 10. From Tables 4.1, 4.4, 4.5 and 4.6 it can be seen that the effect of the magnetic parameter M is to reduce the wall temperature gradient and enhances the skin friction coefficient. While the temperature index parameter n and the Prandtl number enhances the wall temperature gradient for case A and even in the exponential temperature dependency case and shows a slight change in skin friction coefficient. The effect of the stretching parameter β is to enhance both the skin friction coefficient and the temperature gradient as shown in Table 4.1. Numerical solutions of the skin friction coefficient and the heat transfer rate are compared for all the three cases by raising the Prandtl number, for Case B there is an increase in skin friction coefficient while for cases A and C there shows a slight change in the skin friction coefficient but enhances the wall temperature for all cases as shown in table 4.6.

Table 4.1: Comparison of values of $-f''(0)$ and $-\theta'(0)$ for the variation of different parameters for Case A.

Pr	M	β	m	n	<i>bvp4c</i>		shooting method	
					$-f''(0)$	$-\theta'(0)$	$-f''(0)$	$-\theta'(0)$
0.7	0.5		1	1	1.2247449	0.7359575	1.2247449	0.7359598
1	-	-	-	-	1.2247449	0.9408995	1.2247449	0.9408999
3	-	-	-	-	1.2247449	1.8655052	1.2247449	1.8655089
7	-	-	-	-	1.2247449	3.0156515	1.2247449	3.0156577
10	-	-	-	-	1.2247449	3.6645705	1.2247449	3.6645536
0.7	0.1	-	-	-	1.0488089	0.7809371	1.0488089	0.7809368
-	0.2	-	-	-	1.0954451	0.7688642	1.0954451	0.7688642
-	0.3	-	-	-	1.1401754	0.7573781	1.1401754	0.7573781
-	0.4	-	-	-	1.1832161	0.7464244	1.1832161	0.7464243
10	0.5	0	0	-	0.6572368	3.3980941	0.6572367	3.3980357
-	-	1	1	-	1.2247449	3.6645705	1.2247449	3.6645536
-	-	1.33	2	-	1.6042809	3.9535492	1.6042811	3.9535557
-	-	1.6	4	-	2.1732846	4.5054108	2.1732853	4.5054342
-	-	1.75	7	-	2.8192844	5.2449479	2.8192858	5.2449926
1	0.1	1	1	0	1.0488089	0.57191609	1.0488089	0.57191671
-	-	-	-	1	1.0488089	0.98710818	1.0488089	0.98710822
-	-	-	-	2	1.0488089	1.3196013	1.0488089	1.3196031

Table 4.2: Values of skin friction coefficient $Re_x^{1/2}C_f$ and $Re_x^{-1/2}Nu_x$ when Pr=1 compared with previous data.

m	Mustafa [24]		Present results	
	$Re_x^{1/2}C_f$	$Re_x^{-1/2}Nu_x$	$Re_x^{1/2}C_f$	$Re_x^{-1/2}Nu_x$
0	-0.44375	0.44375	-0.44376	0.44376
1	-1.00000	1.00000	-1.00000	1.00000
2	-1.34845	1.34845	-1.34845	1.34845

Table 4.3: Comparison of $Re_x^{-1/2}Nu_x$ for $m = 0$, $n = 0$, $M = 0$, and for various Prandtl numbers to previously published data.

Pr	Jacobi [1] (1993)	Tsou et al. [7] (1969)	Ali [23] (1975)	Present results using bvp4c
0.7	0.3492	0.3492	0.3476	0.3492
1	0.4438	0.44378	0.4416	0.4437
10	1.6790	1.6804	1.6713	1.6803

Table 4.4: Comparison of values of $-f''(0)$ and $-\theta'(0)$ with different values of M at $\beta=1$ for Case B.

M	Pr	β	n	<i>bvp4c</i>		shooting method	
				$-f''(0)$	$-\theta'(0)$	$-f''(0)$	$-\theta'(0)$
0.1	1	1	1	2.5319107	1.2911665	2.5319246	1.2911872
0.2	-	-	-	2.6345052	1.2592202	2.6345262	1.2592542
0.3	-	-	-	2.7320985	1.2297405	2.7321026	1.2297436
0.4	-	-	-	2.8255608	1.2023007	2.8256027	1.2023801
0.5	-	-	-	2.9154891	1.1766242	2.9155451	1.1767366

Table 4.5: Comparison of values of $-f''(0)$ and $-\theta'(0)$ with different values of M and Prandtl number Pr at for Case C.

Pr	M	β	m	n	<i>bvp4c</i>		shooting method	
					$-f''(0)$	$-\theta'(0)$	$-f''(0)$	$-\theta'(0)$
0.7	0.5	1	1	1	1.2253691	1.2372159	1.2253668	1.2372304
1	-	-	-	-	1.2250073	1.5498779	1.2250082	1.5498708
3	-	-	-	-	1.2237208	2.9396428	1.2237234	2.9396226
7	-	-	-	-	1.2226723	4.6632446	1.2226727	4.6632535
10	-	-	-	-	1.2222433	5.6359834	1.2222438	5.6360153
0.7	0	-	-	-	1.0012876	1.3036164	1.0012864	1.3036246
-	0.2	-	-	-	1.0964924	1.2755373	1.0964911	1.2755469
-	0.4	-	-	-	1.1839853	1.2495475	1.1839836	1.2495583
-	0.5	-	-	-	1.2253668	1.2372304	1.2253687	1.2372192
-	1	-	-	-	1.4140959	1.1810374	1.4140974	1.1810246

Table 4.6: Comparison of values of $-f''(0)$ and $-\theta'(0)$ with different Prandtl numbers at $M=0.1$, and $n=1$.

			<i>bvp4c</i>		shooting method	
Cases	M	Pr	$-f''(0)$	$-\theta'(0)$	$-f''(0)$	$-\theta'(0)$
CaseA	0.1	0.7	1.0488089	0.7809371	1.0488089	0.7809368
CaseB			2.4815005	0.9823335	2.4815331	0.9824429
CaseC			1.0499816	1.2892992	1.0499833	1.2892871
CaseA	0.1	1	1.0488089	0.98710818	1.0488089	0.98710822
CaseB			2.5319127	1.2911679	2.5319324	1.2911909
CaseC			1.0495539	1.6009485	1.0495531	1.6009555
CaseA	0.1	10	1.0488088	3.7084904	1.0488088	3.7084992
CaseB			3.1938761	5.5.2855821	3.1938595	5.285655
CaseC			1.0467705	5.6811359	1.0467682	5.6811186

Three cases have been discussed to study the effect of temperature-dependent viscosity. The ambient fluid is considered at temperature $T_0 = 278\text{K}$ and the surface temperature is taken as $T_w = 358\text{K}$. Figs. 4.1 and 4.2 show the effect of Prandtl number for three different cases A, B and C. The velocity profile in Fig. 4.1 is reduced near the moving surface for case B as compared to the other two cases A and C which gave the exact same result for the momentum boundary layer thickness. The surface heats the adjacent fluid and thereby reduces its viscosity. The temperature profile in Fig. 2 is reduced near the moving surface for case A and case C as compared to case B. The influence of magnetic parameter M on velocity and temperature profiles is shown in Figs. 4.3-4.8. The increase in M causes an increase in temperature profile while shows the reduction in the thickness of momentum boundary layer due to increase in M parameter for all cases.

The effect of the stretching parameter β on the velocity profile in the presence of the magnetic parameter M is depicted in Figs. 4.9-4.13. It is observed that an increase in the stretching parameter β reduces the momentum boundary layer thickness, whereas the thermal boundary layer also reduces for cases A and C but for the case B it increases. Physically, $\beta > 0$ implies the surface accelerating case. Figs. (4.14-4.16) shows samples of the dimensionless velocity and temperature profiles as a function of the similarity variable η for various values of temperature index parameter n . The increase in n parameter causes a decrease in the thickness of thermal boundary layer for case A and C while there is an increasing effect in the momentum boundary layer thickness for case B. The effect of variation of Prandtl number is shown in Figs. (4.17-4.20). In Fig. 4.19, for case B there is an increase in the momentum boundary layer with an increase in Prandtl number while the thermal boundary layer thickness for all cases reduces by raising the Prandtl number but has no such effect on velocity profile for case C.

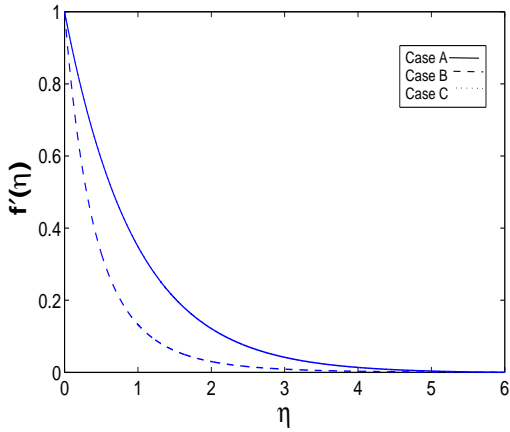


Figure 4.1: Velocity profile for different cases (A, B and C) at $Pr = 0.7, n = 1$ and $M, \epsilon = 0.1$.

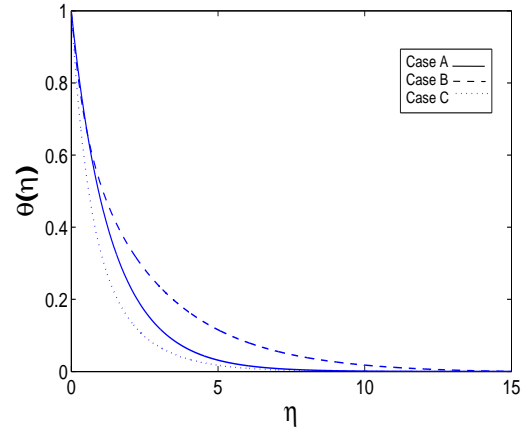


Figure 4.2: Temperature profiles for different cases (A, B and C) at $Pr = 0.7, n = 1$ and $M, \epsilon = 0.1$.

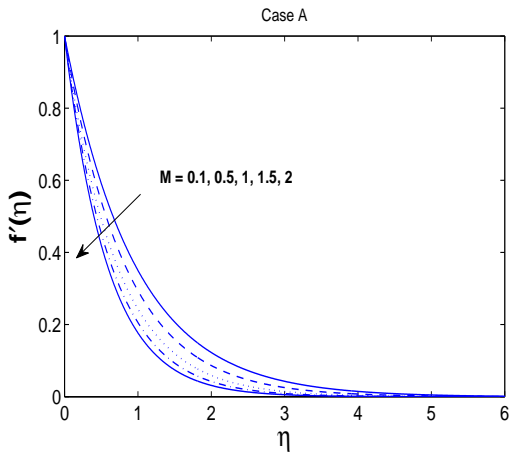


Figure 4.3: Velocity profiles for different values of magnetic parameter M with $n = 1, \beta=1$ and $Pr=0.7$.

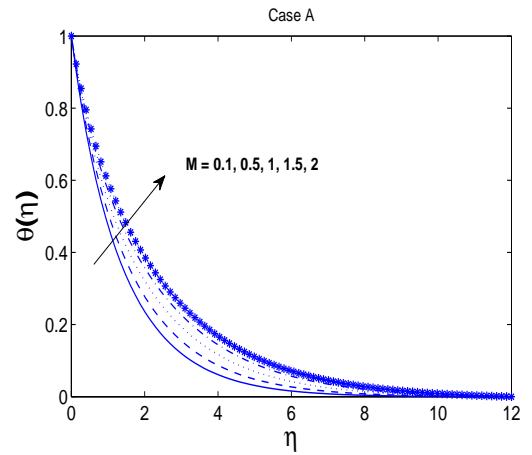


Figure 4.4: Temperature profiles for different values of magnetic parameter M with $n = 1, \beta=1$ and $Pr=0.7$.

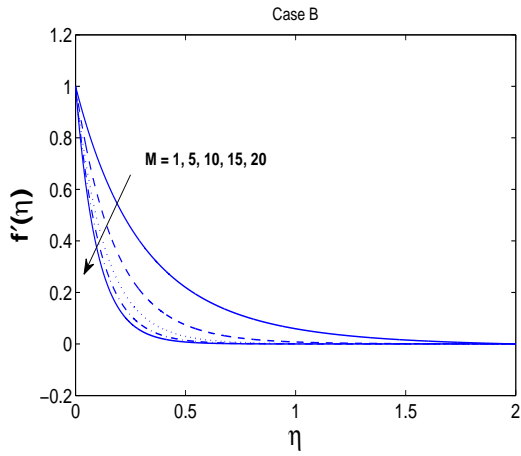


Figure 4.5: Velocity profiles for different values of magnetic parameter M with $n = 1$, $\beta=1$ and $Pr=0.7$.

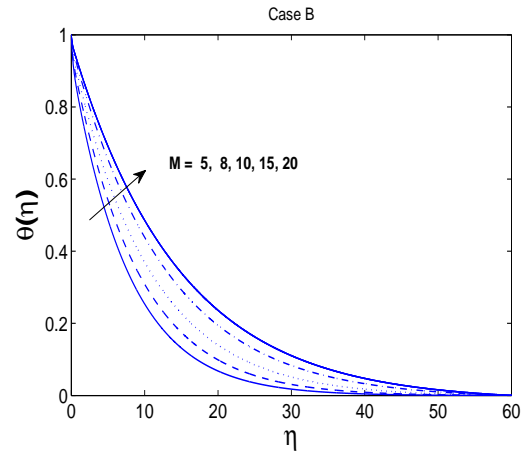


Figure 4.6: Temperature profiles for different values of magnetic parameter M with $n = 1$, $\beta=1$ and $Pr=0.7$.

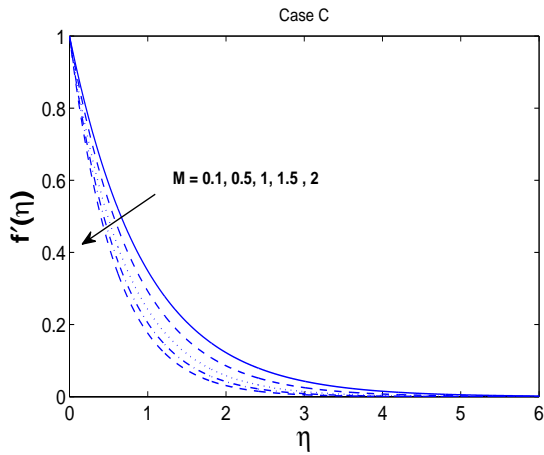


Figure 4.7: Velocity profiles for different values of magnetic parameter M with $n = 1$, $\beta=1$ and $Pr=0.7$.

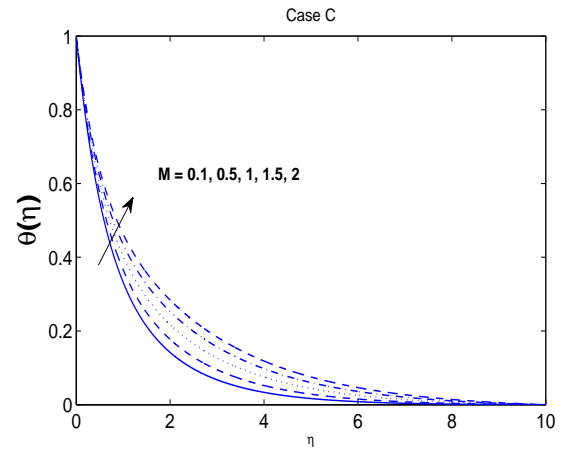


Figure 4.8: Temperature profiles for different values of magnetic parameter M with $n = 1$, $\beta=1$ and $Pr=0.7$.

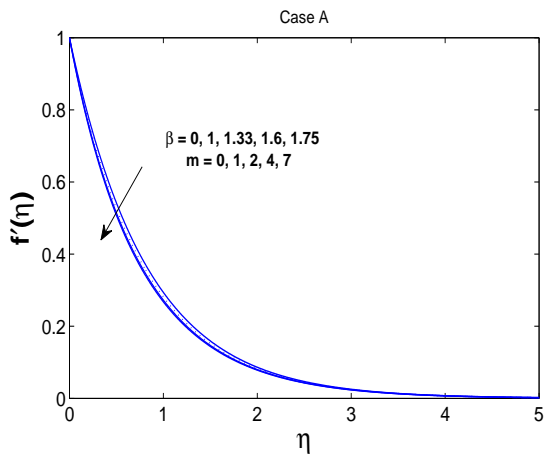


Figure 4.9: Velocity profiles for different values of parameter β with $n = 1$, $M = 0.5$ and $Pr=0.7$.

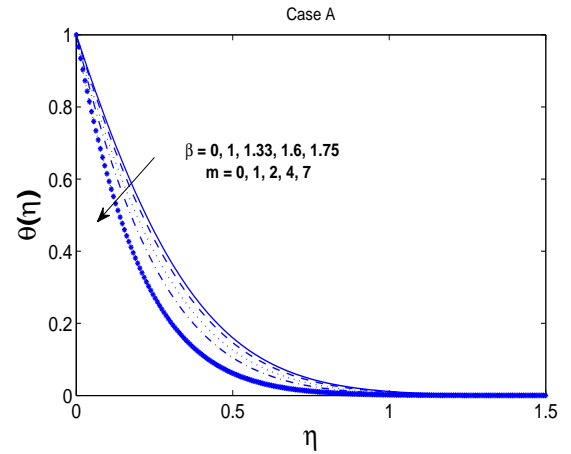


Figure 4.10: Temperature profiles for different values of parameter β with $n = 1$, $M = 0.5$ and $Pr=10$.

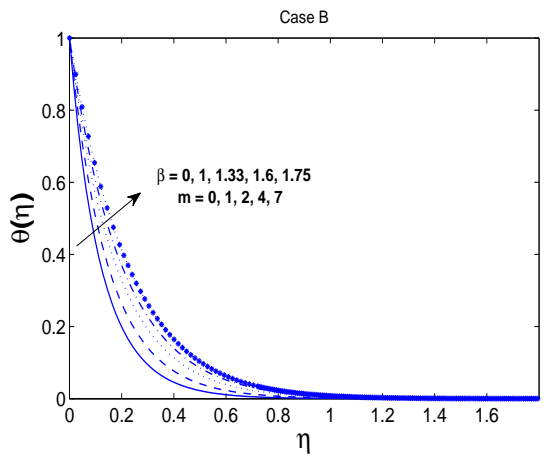


Figure 4.11: Temperature profiles for different values of parameter β with $n = 1$, $M = 0.5$ and $Pr=10$.

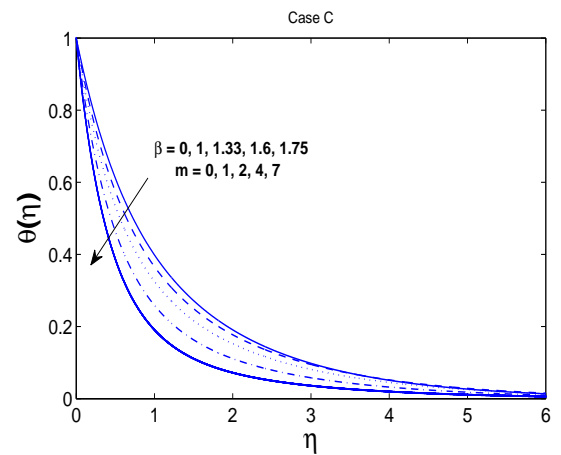


Figure 4.12: Temperature profiles for different values of parameter β with $n = 1$, $M = 0.5$ and $Pr=0.7$.

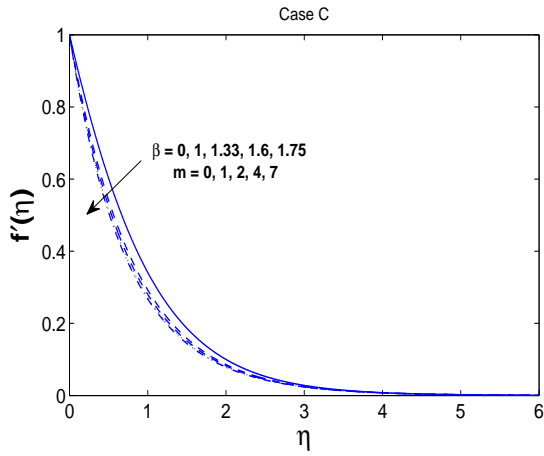


Figure 4.13: Velocity profiles for different values of parameter β with $n = 1$, $M = 0.5$ and $Pr=0.7$.

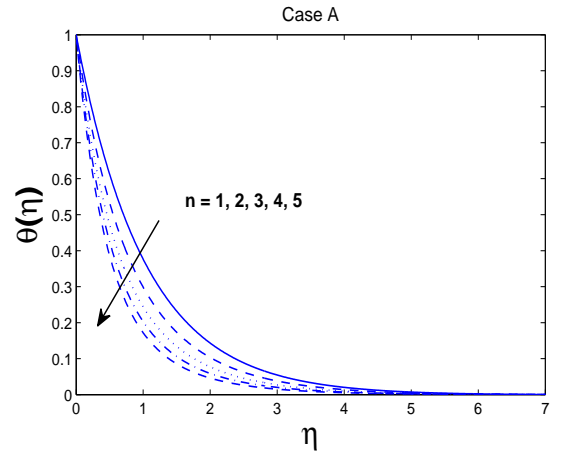


Figure 4.14: Temperature profiles for different values of temperature index parameter n with $M = 0.1$, $m = 1$ and $Pr=1$.

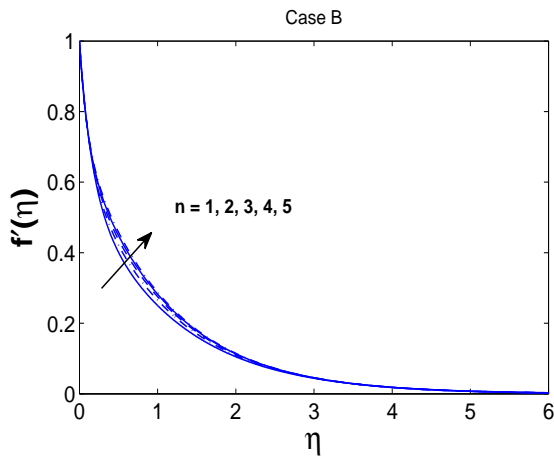


Figure 4.15: Velocity profiles for different values of temperature index parameter n with $M = 0.1$, $m = 1$ and $Pr=10$.

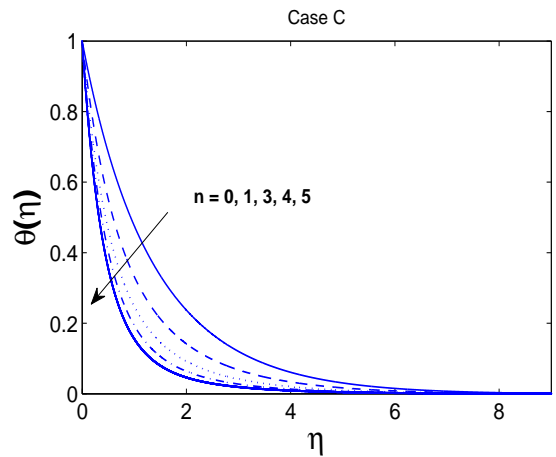


Figure 4.16: Temperature distribution for various values of temperature index parameter n with $M = 0.1$, $m = 1$ and $Pr=0.7$.

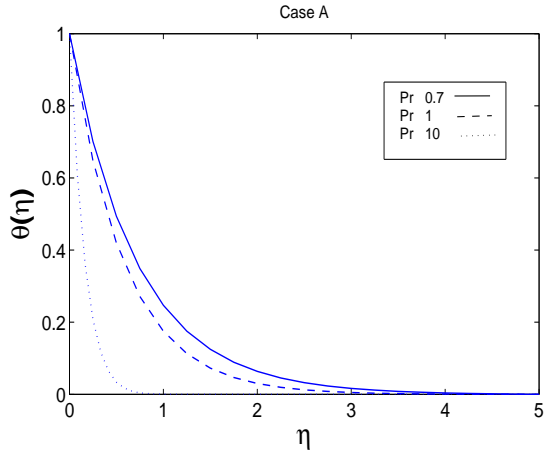


Figure 4.17: Temperature profiles for different values of Pr at $M=0.1$.

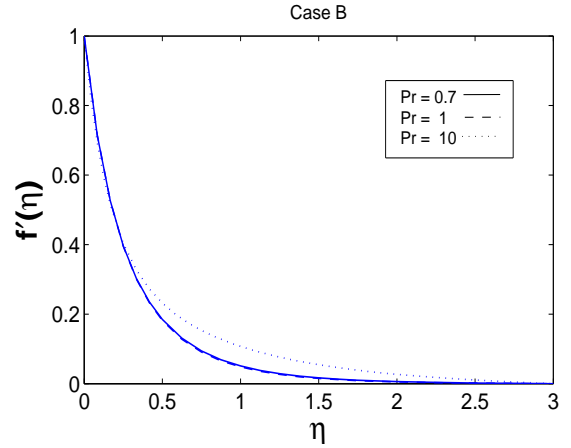


Figure 4.18: Velocity profiles for different values of Pr at $M=0.1$.

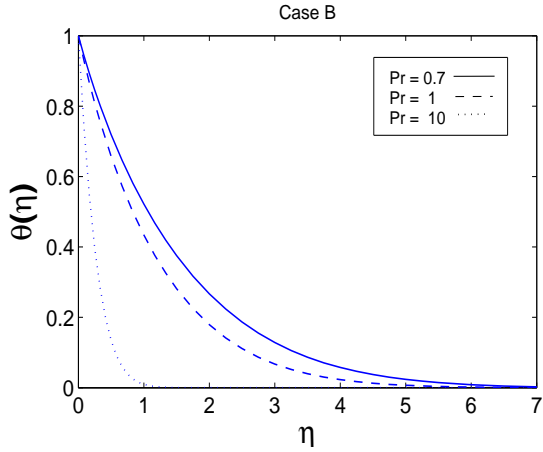


Figure 4.19: Temperature profiles for different values of Pr at $M=0.5$.

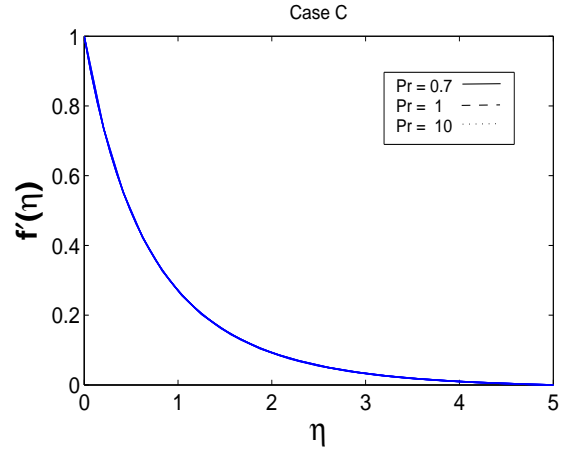


Figure 4.20: Velocity profiles for different values of Pr at $M=0.5$.

4.6 Concluding Remarks

The effect of the magnetic parameter is to increase the skin friction coefficient and the thermal boundary layer thickness and reduces the velocity profile and the wall temperature. The momentum and thermal boundary layer thickness are reduced by the stretching parameter β for the cases, but for the case B, the thermal boundary layer increases. While the effects of stretching parameter are to increase the both skin friction coefficient and the temperature gradient. It is observed, the effect of Prandtl number shows a slight change in the skin friction

and momentum boundary layer thickness but enhances the wall temperature and shows an increasing effect in momentum boundary layer thickness for variable viscosity case. By raising the Prandtl number, it reduces the thermal boundary layer thickness. The increase in temperature index parameter n resulted in a decrease in momentum boundary layer thickness as well as in the thickness of thermal boundary layer but for variable viscosity case the momentum boundary layer thickness and the wall temperature increases.

Chapter 5

Conclusion and Outlook

In this chapter, we have drawn the conclusion of all the results that have been computed in the previous chapters and also discussed the work that can be further extended in future.

In this dissertation, we have studied the variable fluid properties. We have mainly focused on the phenomenon of viscosity as a function of temperature. The MHD boundary layer flow and heat transfer of a viscous fluid over a linear and nonlinear stretching sheet with variable fluid properties are also presented. In our study, various cases are discussed including the constant properties of the fluid and the variable viscosity along with the exponential case on a temperature dependency of the fluids to analyze the MHD flow and the transfer of heat characteristics over the stretching surface. The surface is stretched linearly as well as nonlinearly to analyze the MHD boundary layer flow.

The effects of different parameters such as magnetic parameter M , velocity exponent m , temperature index parameter n , stretching parameter β , velocity ratio parameter ϵ , and Prandtl number Pr on the MHD flow and heat transfer characteristics are investigated. The various numerical results for different parametric conditions are obtained graphically for the velocity and temperature profiles. The system of the governing boundary layer equations developed along with the boundary conditions. A special type of transformations is used known as the similarity transformation to reduce the system of the governing boundary layer equations into a coupled system of nonlinear ODEs. Different numerical results have been computed by using the shooting method. These computed results are compared with literature and

some new results are presented.

In future, we can further extend this work by taking into account not only the density but also the thermal conductivity as a linear function of temperature. As in our case, we focus on the viscosity as a temperature dependent only. One can pursue this work by considering the temperature dependent fluid properties like density etc. This work can also be extended for an exponential stretching sheet

As we used the shooting technique and *bvp4c* algorithms to solve the BVPs, one can try other numerical algorithms like FDM, to compute the results. In practical applications the usage of the shooting technique to solve the BVP is quite beneficial as the error found by this method is very small as compared to other numerical schemes, and it also gives approximately the same result.

Bibliography

- [1] A. M. Jacobi, A scale analysis approach to the correlation of continuous moving sheet (backward boundary layer) forced convective heat transfer *J. Heat Transfer*, **115** (1993), 1058-1061.
- [2] A. Chakrabarti and A.S. Gupta, Hydromagnetic flow and heat transfer over a stretching sheet, *Quart. Appl. Math.*, **37** (1979) 73-78.
- [3] A. Pantokratoras, Further results on the variable viscosity on flow and heat transfer to a continuous moving flat plate, *Int. J. Eng. Sci.*, **42** (2004) 1891-1896.
- [4] A. Ishak, K. Jafar, R. Nazar, I. Pop, MHD stagnation point flow towards a stretching sheet, *Phys A: Stat. Mech. Appl.* (2009) **388** (17) 3377-3383.
- [5] B. C. Sakiadis, Boundary-layer behaviour on continuous solid surfaces. The Boundary-layer flow on a continuous at surface, *J. Appl. Math.*, **7** (1961) 221-225.
- [6] E. M. A Elbashbeshay and M. A. A. Bazid, The effect of temperature-dependent viscosity on heat transfer over a continuous moving surface, *J. Phys. D: Appl. Phys.*, **33** (2000) 2716-2721.
- [7] F.K. Tsou, E.M. Sparrow and R.J. Goldstein, Flow and heat transfer in the boundary layer on a continuous moving surface, *Int. J. Heat Mass Transfer*, **10** (1967),219- 235.
- [8] F. C. Lai and F. A. Kulacki, The effect of variable viscosity on convective heat transfer along a vertical surface in a saturated porous medium, *Int. J. Heat Mass Transfer* **33**, 1990 1028-1031.

- [9] F.M. White, *Viscous Fluid Flow*, (third ed.) McGraw-Hill, New York (2006).
- [10] F. M. Ali, R. Nazar, N. M. Arifin and I. Pop, MHD mixed convection boundary layer flow toward a stagnation point on a vertical surface with induced magnetic field, *J. Heat Transfer* **133** (2011) Article ID: 022502-1-6.
- [11] Google image, <https://scienceofdoom.com/2011/01/02/heat-transfer-basics-convection-part-one>.
- [12] H. Blasius, Grenzschichten in flüssigkeiten mit kleiner reibung, *Z. Angew. Math. Phys.*, (1908) 1-37.
- [13] H. I. Andersson and B. S. Dandapat, Flow of a power-law fluid over a stretching sheet, *Stability Appl. Anal. Continuous Media* **1** (1991) 339-347.
- [14] H. I. Andersson, K. H. Bech and B. S. Dandapat, Magnetohydrodynamic flow of a power-law fluid over a stretching sheet, *Int. J. Non-Linear Mechanics.* **27** (1992) 929-936.
- [15] H. Andersson and J. Aarseth, Sakiadis flow with variable fluid properties revisited, *Int. J. Eng. Sci.*, **45** (2007) 554-561.
- [16] I. Pop, R. S. R. Gorla and M. Rashidi , The effect of variable viscosity on the flow and heat transfer to a continuous moving flat plate, *Int. J. Eng. Sci.* **30** (1992) 1-6.
- [17] J. X Ling and A. Dybbs, Forced convection over a flat plate submersed in a porous medium:variable viscosity case, *Am. Soc. Mech. Eng.* **114**, (1987) 87-123.
- [18] K. B. Pavlov, Magnetohydrodynamic flow of an incompressible viscous fluid caused by deformation of a plane surface, *Magnitnaya Gidrodinamika (U.S.S.R.)*, **4** (1974) 146-147.
- [19] K. V. Prasad, K. Vajravelu and P. S. Datti, The effects of variable fluid properties on the hydro-magnetic flow and heat transfer over a non-linearly stretching sheeta stretching sheet. *Int. J. Thermal Sci.* **49** (2010) 603-610.
- [20] L. J. Crane, Flow past a stretching plane, *Z. Angew. Math. Phys.*, **21** (1970) 645-647.

- [21] Lawrence F. Shampine, Jacek Kierzenka and Mark W. Reichelt, Solving boundary value problems for ordinary differential equations in matlab with bvp4c, CEM-UVM, (2000).
- [22] M. E. Ali, Heat transfer characteristics of a continuous stretching surface, *Warme Stoffubert*, **29** (1994) 227-234.
- [23] M. E. Ali, On thermal boundary layer on a power law stretched surface with suction or injection, *Int. J. Heat Mass Flow*, **16** (1995), 280 -290.
- [24] M. Mustafa, Viscoelastic flow and heat transfer over a non-linearly stretching sheet: OHAM solution, *J. Appl. Fluid Mech.*, **9** (2016) 1321-1328.
- [25] N. Afzal, I. S. Varshney, The cooling of a low heat resistance stretching sheet moving through a fluid, *WÄdrme- und StoffÄijbertrag* **14** (1980) 289-293.
- [26] N. Afzal, Heat transfer from a stretching surface, *Int. J. Heat Mass Transfer*, **36** (1993) 1128-1131.
- [27] N. Bachok, A. Ishak and I. Pop, Boundary layer flow and heat transfer with variable fluid properties on a moving flat plate in a parallel free stream, *J. Appl. Math.* **2012** (2012), Article ID 372623, 10 pages.
- [28] O. D. Makinde, W. A. Khan, and J. R. Culham, MHD variable viscosity reacting flow over a convectively heated plate in a porous medium with thermophoresis and radiative heat transfer, *Int. J. Heat Mass Transfer*, **93** (2016) 595-604.
- [29] S. Mukhopadhyay, G. C. Layek and Sk. A. Samad, Study of MHD boundary layer flow over a heated stretching sheet with variable viscosity, *Int. J. Heat Mass Transfer*, **48** (2005) 4460-4466.
- [30] T. Fang, F. Guo, and Chia-f. F. Lee, A note on the extended Blasius equation, *Applied Mathematics* **19** (2006) 613-617.
- [31] T. M. Agbaje, S. Mondal, Z.G. Makukula, S.S. Motsa and P. Sibanda, A new numerical approach to MHD stagnation point flow and heat transfer towards a stretching sheet, *Ain Shams Eng. J.* (2015).